CFD Letters

Journal homepage:
https://semarakilmu.com.my/journals/index.php/CFD_Letters/index
ISSN: 2180-1363

Study of MHD Casson Nanofluid Flow over an Inclined Stretching Sheet in Porous Media with Thermal Slip, Chemical Reaction and Radiation Effects

Aruna Ganjikunta[1], Ramanjana Koka[2,*]

[1] Department of Mathematics, School of Science, GITAM-Hyderabad Campus, Hyderabad 502 329, Telangana, India
[2] Department of Mathematics, St. Francis College for Women, Begumpet, Hyderabad-500 016, Telangana, India

ARTICLE INFO

Article history:
Received 24 March 2024
Received in revised form 21 April 2024
Accepted 20 May 2024
Available online 31 October 2024

Keywords:
Inclined Stretching Sheet;
Radiation; Chemical Reaction;
Heat Generation; Magnetic field;
Porous medium

ABSTRACT

In the current study, the behaviour of Casson nanofluid subjected to magnetohydrodynamic (MHD) flow across an inclined stretched sheet within a porous medium has been investigated numerically. The governing equations are transformed into ordinary differential equations with the corresponding boundary conditions by employing similarity transformations. The solutions of essential equations are achieved by using the 4th-order Runge-Kutta method combined with the shooting technique. The novelty and innovative contribution are showcased through illustrative graphs that scrutinize the effect of factors that impact the velocity, temperature, and concentration profiles within assorted flow scenarios. The primary focal points of the study encompass examining variations in magnetic field strength, angle of inclination, and suction intensity that affect the fluid's velocity moderation, while improved porosity and radiation parameters lead to a rise in fluid temperature. Higher Biot numbers correlate with an increase in fluid temperature. The implications of positive coefficients of heat transfer are crucial across various fields to ensure efficient thermal management ensuring optimal performance and longevity. The numerical data presented is aligned with earlier published results for comparison. Furthermore, the variations in skin friction, Nusselt, and Sherwood numbers driven by different parameters are displayed in tables to highlight significant modifications.

1. Introduction

Research on the magnetohydrodynamic (MHD) flow of Casson nanofluid across an inclined stretching sheet has been applied in a wide array of sectors, including industrial operations, biomedical engineering, exploration of oil and gas, processing of materials, manufacturing, and environmental engineering. It offers insightful information on how complicated fluid-solid mixes behave when surface inclination and magnetic fields are coupled, which facilitates the creation of cutting-edge technologies and solutions to various technical problems. In their research, Choi *et al.,* [1] proposed a novel class of heat transfer through dispersion of nanoparticles within conventional heat transfer fluids. Gupta U *et al.,* [2] used blood as the basis fluid and studied the instability of

* *Corresponding author.*
E-mail address: rkoka@gitam.in (Ramanjana Koka)

https://doi.org/10.37934/cfdl.17.3.167195

Casson binary nanofluids analytically and numerically. Upreti *et al.,* [3] studied the characteristics of heat and mass transfer in 3D (three-dimensional) flow of Casson nanofluid comprising gyrotactic microorganisms over a Riga plate. In their work, Ibrahim *et al.,* [4] examined the impact of slip and convective boundary conditions over heat transfer through MHD processes caused by Casson nanofluid flowing past a stretched sheet. Numerous investigators have delved into the intricacies of magnetohydrodynamics (MHD) fluid flows. Among them are Wan *et al.,* [5], Khan Ansab *et al.,* [6], Raghunath *et al.,* [7], Mopuri *et al.,* [8], Reddy Yanala *et al.,* [9], Vishwanatha *et al.,* [10], and Bejawada *et al.,* [11] who have each contributed to this area with their respective research endeavours. Kodi R *et al.,* [12] presented an in-depth analytical analysis of flow characteristics of Casson fluid, which include mass and heat transfer, in an unstable convective magnetohydrodynamic environment under the impact of chemical reactions and thermal diffusion. Gangadhar *et al.,* [13] examined the existence of dual solutions in MHD flow of a Casson fluid interaction within a porous shrinking surface. Using the Casson model, Koka R *et al.,* [14] investigated the MHD flow across a linearly stretching sheet in a porous media. Senapati *et al.,* [15] explored by using the Casson fluid model how blood flows in narrow arteries. Malik *et al.,* [16] analysed the heat transfer in a Casson nanofluid, flowing around an oriented cylinder. Tawade *et al.,* [17] examined heat transfer on a linear stretching sheet to study the flow behaviour of a Casson nanofluid in a 2D (two-dimensional) boundary layer. Jamshed Wasim *et al.,* [18], in their article, used the Tiwari-Das nanofluid model to delve into the magnetohydrodynamic (MHD) secretion of secondary fluid within an expanded region.

Inclined stretching sheets are valuable experimental tools for exploring various aspects of fluid dynamics, including turbulent flows, heat transfer mechanisms; shear flow characteristics, boundary layer phenomena, and numerical validation. Their practical utility extends across disciplines such as physics, engineering, and environmental sciences, providing valuable insights into the fundamental principles governing fluid motion. Khan W.A *et al.,* [19] numerical investigation into the laminar fluid flow phenomenon when a flat surface is stretched in a nanofluid. This study marks the pioneering exploration of on-sheet stretching in nanofluids. Unravelling the interplay between slip and transport, Usman M *et al.,* [20] delved into how velocity and thermal variation at the interface influence Casson nanofluid's heat and mass transport phenomena flowing around an inclined permeable stretched cylinder. Bharathi *et al.,* [21] explored the convection of transient states in MHD Casson fluid flow across an inclined layer considering the Dufour effects and heat suction or injection past porous media. Alabdulhadi *et al.,* [22] investigated heat transfer and unstable thin-film Al_2O_3 water nanofluid flow through an inclined stretching sheet with a buoyancy force effect. Also, Biswal *et al.,* [23] emphasized the boundary layer stagnation-point flow in the direction of a nonlinearly inclined stretched sheet immersed in a porous medium using MHD. Barik *et al.,* [24] investigated the magnetohydrodynamic (MHD) properties of an electrically conducting nanofluid passing by an inclined stretching sheet numerically. Rehman *et al.,* [25] unveiled a mathematical model for the Casson fluid flow over an unstable stretched sheet under the influence of natural factors and heat transmission, including suction and injection phenomena. In their article, Mishra *et al.,* [26] examined the MHD flow of viscous fluid travelling through a stretched surface vulnerable to induced magnetic field effects and heat radiation. Endalew *et al.,* [27] explored mass transfer and thermal properties that influence the movement of an isotropic incompressible Casson fluid across an oscillating plate considering thermal and solutal boundary conditions.

A porous medium is an element or component with interconnected empty spaces or pores that allow fluids such as gases or liquids to move through it. The physical characteristics of porous media, such as their pores' dimensions, shapes, and interconnections, significantly influence their overall behaviour, encompassing fluid dynamics and conveyance of heat and mass. The magnetic field plays a vital role in numerous science and technology domains. Its influence can affect the alignment and

conduct of magnetic particles, materials, or fluids. This alignment of magnetic fields in fluids has diverse and vital applications, managing and influencing fluid movement and conduct in various settings. This has far-reaching consequences in fluid dynamics, enabling the advancement of novel technologies for power generation, propulsion, and plasma regulation.

Incorporating porous medium and magnetic fields into fluid dynamics models opens various applications such as Magnetic Drug Targeting, Enhanced Oil Recovery, Magnetic Filtration, Magnetic Cooling Systems, and Magnetohydrodynamics (MHD) Power Generation. These applications demonstrate the broad spectrum of disciplines where integrating porous media and magnetic fields can significantly advance technology, medicine, and environmental sustainability. Sarwar *et al.,* [28] investigated the flow dynamics of Casson nanofluid with an inherent slip under an angled magnetic field and guided over a non-linear stretched sheet. Manvi *et al.,* [29] provided a numerical investigation of Casson nanofluids flowing through porous materials on stretched magnetic surfaces. Panigrahi *et al.,* [30] investigated the effects of an inclined magnetic field on the flow of Casson nanofluid over a stretched surface embedded in a saturated porous medium, focusing on impacts of variable heat source/sink and thermal radiation. In their study, Raza *et al.,* [31] compared thermal properties of nanofluids subjected to an angled magnetic field, using kerosene oil and water base fluid as examples where the sloping surface caused the flow. Inside the framework of local thermal non-equilibrium (LTNE) circumstances, Koka R *et al.,* [32] studied the behaviour of Casson nanofluid fluid over a stretching sheet, specifically focusing on the effects of porosity and an aligned magnetic field with the flow. Mahabaleshwar *et al.,* [33] showcased axisymmetric stagnation flow of Casson nanofluid (consists of water with Fe_3O_4 nanoparticles) within a laminar boundary layer passing over a stretching plate subject to the influence of suction/injection and heat radiation.

The complex interrelations involving the magnetic field, heat radiation, thermophoresis, and Brownian motion within a porous medium over an inclined stretching surface are contingent upon several factors, such as the intensity of the magnetic field, the properties of the fluid, and the composition of the porous medium. Understanding the effects of these interactions is crucial for enhancing processes and applications in scenarios where such flow conditions occur. The real-time applications include fluid dynamics, material processing, and environmental engineering. Suresh Kumar *et al.,* [34] examined the behaviour of the Casson nanofluid in terms of flow, heat, and mass transfer via an exponentially extending surface considering the impacts of thermophoresis, Brownian motion, thermal radiation, activation energy, and Hall current. Noghrehabadi *et al.,* [35] investigated the influence of slip effects on heat transfer and boundary layer flow over a stretched surface in the presence of nanoparticle fractions, and thermophoresis and Brownian motion are two dynamic processes considered in nanofluid modelling. Sekhar *et al.,* [36] applied the Buongiorno model to study the thermal efficiency of Casson Nanofluid flow over an inclined stretched surface. Jayalakshmi *et al.,* [37] delved into the characteristics of the 3D flow of a Sisko fluid over a bidirectional stretching surface in the presence of Lorentz force. Vyakaranam *et al.,* [38] examined the effects of radiation with a synthetic response, as well as the relevance of thermophoresis dispersion and Brownian movement on MHD flow Casson nano liquid via a nonlinear slanted permeable extending surface. Roja *et al.,* [39] in their study recorded thermal radiation and thermophoresis associated with a stable magnetohydrodynamic free convection stream of a micropolar liquid via an upright porous laminate.

Nagaraja *et al.,* [40] numerically analysed dusty nanofluid streams on a stretched sheet under thermal radiation, melting heat, and slip conditions. Odesola *et al.,* [41] studied heat transfer of Casson-Carreau nanofluid flow across a stretched surface, analysing the influence of radiation, internal heat generation, and heat dissipation. Hayat *et al.,* [42] conferred the boundary layer flow of a Casson fluid due to a stretched cylinder with heat radiation effects. Heat Transport in 2D MHD

Systems by Ramesh *et al.,* [43] employs mathematical models of flow problems, such as heat absorption/generation and the Cattaneo-Christov heat diffusion theory, to articulate Casson fluid flow. Reddy Nalivela Nagi *et al.,* [44] examined how porosity affects unsteady magnetohydrodynamics mixed convection heat and mass transfer flow at the stagnation point with radiation and viscous dissipation. In their study, Madhu *et al.,* [45] examined continuous 2D MHD flow of Casson nanofluid over a wedge while accounting for thermophoresis and Brownian motion impacts. Pal *et al.,* [46] conducted a computational analysis of the MHD boundary layer flow of Casson nanofluid over a vertically stretching surface, which featured non-linear stretching velocity and suction. They encompassed the effects of thermophoresis, Brownian motion, thermal radiation and Ohmic dissipation. Al-Mamun *et al.,* [47] described a non-Newtonian fluid flow of the Casson type towards a stretched surface by mass conduction and heat, with the effects of thermophoresis and radiation absorption on the periodic hydromagnetic effect.

Considering chemical reactions in fluid dynamics is critical for various applications, including combustion, chemical processing, environmental engineering, and biochemical processes. By incorporating these parameters into mathematical models, engineers and scientists can predict and optimize the behaviour of fluids when chemical reactions are involved. Ghadikolaei *et al.,* [48] provided a numerical analysis and exploration of mixed convective MHD flow of Casson nanofluid through a stretching sheet with non-linear permeability with the effects of chemical processes and Joule heating by incorporating Buongiorno's model. With similar results, Rafique K *et al.,* [49] also analysed the impacts of chemical reactions by employing the Buongiorno model. Bhandari *et al.,* [50] examined the MHD flow behaviour of Casson nanofluid around a shrinking and stretching cylinder, emphasizing the effects of chemical reactions. Patil *et al.,* [51] examined characteristics of a chemical reaction and MHD Prandtl nanofluid flow over a stretched sheet, focusing on convective boundary conditions. Jain *et al.,* [52] analysed heat transfer dynamics of MHD Casson nanofluid flow over a non-linear stretching sheet by incorporating velocity and temperature slip boundary conditions within the framework of the chemical reaction. Kumar Vasa *et al.,* [53] explored numerical solutions addressing the complexities of heat generation and chemical reaction within a saturated porous material involving a transverse magnetic field. Kumar *et al.,* [54] investigated the Soret-Dufour phenomena influencing the behaviour of an unstable, viscous, and incompressible magnetohydrodynamic (MHD) flow, considering the effects of chemical reactions.

The main aim of this study is to investigate how the interplay of heat and mass buoyancy forces, along with thermal slip, affects the dynamics of a steady, incompressible laminar flow of Casson nanofluid over an inclined stretching sheet embedded in a porous medium while considering the influence of magnetic fields. Additionally, the study examines the influences of heat generation, radiation, thermophoresis, Brownian motion, and other relevant parameters on the flow characteristics.

The research delineates potential applications across industries that offer insights into the growth of polymer processing, drug delivery systems, solar collectors, and groundwater remediation processes, understanding the flow behaviour of complex fluids which is crucial for quality control and process optimization.

The objective of this research lies in its extension of previous studies by incorporating magnetic field, porous medium, radiation, heat generation, and chemical reaction effects along with heat and mass buoyancy forces coupled with thermal slip into the governing equations. A comparison has been made with previous results to measure the assurance of achieving similar outcomes from the produced results. Figure 1 provides a visual description of flow geometry.

2. Mathematical Formulation

Considering a 2D steady incompressible, laminar, magnetohydrodynamics (MHD) flow of a Casson nanofluid across an inclined permeable stretching sheet at an angle $\alpha(0 < \alpha < 90°)$ (inclined angle) from its vertical axis in a homogeneous porous medium. Figure 1, shows the physical model and coordinate system in which x-axis aligned along the inclined surface and the y -axis is placed normal to the surface, as shown in Figure 1. The flow is taken in the x-direction and restricted to $y > 0$. The velocity at which the sheet is stretched is given by

$$u_w(x) = ax$$

Where $'a'$ represents a stretching constant. The magnetic field B_o is applied at a right angle to the $x-$ axis and the entire fluid domain. v_w signifies, blowing velocity at the wall.

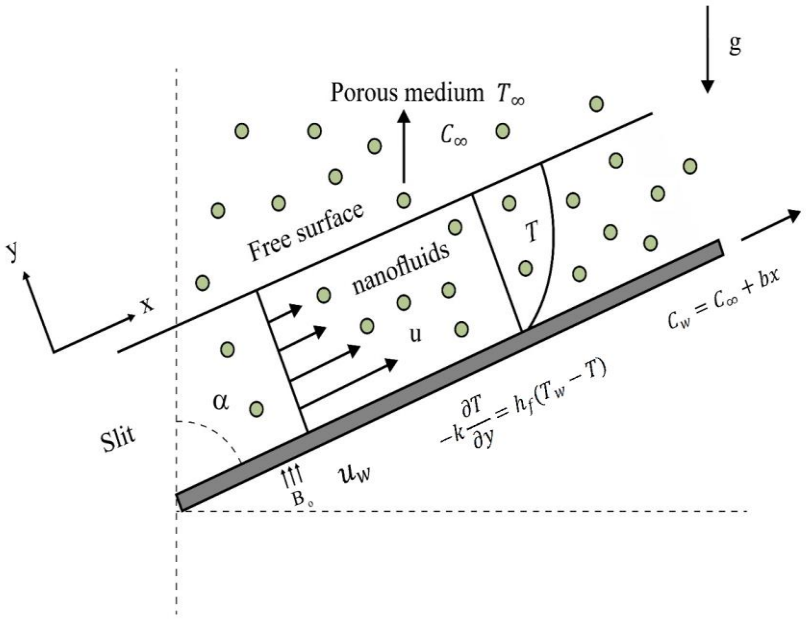

Fig. 1. Flow Geometry Alabdulhadi *et al.,* [22]

For the flow of a Casson fluid that is isotropic and incompressible, the rheological equation of state is provided as taken from a previous study by Yusof Nur *et al.,* [55].

$$\tau_{ij} = \begin{cases} 2\left(\mu_B + \frac{P_y}{\sqrt{2\pi}}\right)e_{ij}, \pi > \pi_c \\ 2\left(\mu_B + \frac{P_y}{\sqrt{2\pi_c}}\right)e_{ij}, \pi_c > \pi \end{cases}$$

Here $\pi = e_{ij}e_{ij}$ is a rate of deformation multiplied by itself, e_{ij} is $(i,j)^{th}$ component of deformation rate, with itself, μ_B is non-Newtonian fluid's plastic dynamic viscosity, P_y is fluid's yield stress, and π_c signifies critical value followed by a non-Newtonian model.

For $\pi_c > \pi$, we get $\tau_{ij} = 2\mu_B \left(1 + \frac{1}{\beta}\right) e_{ij}$; where $\beta = \mu_B \frac{\sqrt{2\pi_c}}{P_y}$ is Casson parameter.

In the current study, the Casson nanofluid flow is altered by the effects of radiation, heat generation, chemical reactions and buoyancy on the velocity, temperature, and concentration profiles. A thermal slip is considered at the bounding surface and the fluid temperature. Also, chemically reactive diffusive species exhibit varying concentrations at the surface considered.

The temperature of the fluid T (K) and concentration C at the stretching surface are represented as T_w and C_w, respectively. The free stream temperature and free stream concentration are represented by T_∞ (K) and C_∞ respectively.

Due to heat generation implications along chemical processes over an inclined stretching sheet inside boundary layer approximations, the governing equations for this problem are categorized into four sections: the equations for the conservation of mass, momentum, energy, and concentration are provided below as taken from previous studies by Tawade *et al.,* [17],

$$\frac{\partial u}{\partial x} + \frac{\partial v}{\partial y} = 0 \tag{1}$$

$$u\frac{\partial u}{\partial x} + v\frac{\partial u}{\partial y} = \vartheta\left(1 + \frac{1}{\beta}\right)\frac{\partial^2 u}{\partial y^2} + g\beta_T(T - T_\infty)\cos\alpha + g\beta_C(C - C_\infty)\cos\alpha - \frac{\sigma {B_o}^2}{\rho_f}u - \frac{\vartheta}{K^{**}}u \tag{2}$$

$$u\frac{\partial T}{\partial x} + v\frac{\partial T}{\partial y} = \alpha^*\frac{\partial^2 T}{\partial y^2} + \tau\left[D_B\frac{\partial C}{\partial y}\frac{\partial T}{\partial y} + \frac{D_T}{T_\infty}\left(\frac{\partial T}{\partial y}\right)^2\right] - \frac{1}{(\rho c)_f}\frac{\partial q_r}{\partial y} + \frac{Q}{(\rho c)_p}(T - T_\infty) \tag{3}$$

$$u\frac{\partial C}{\partial x} + v\frac{\partial C}{\partial y} = D_B\frac{\partial^2 C}{\partial y^2} + \frac{D_T}{T_\infty}\frac{\partial^2 T}{\partial y^2} - K_0(C - C_\infty) \tag{4}$$

As radiative heat flux is considered much small than that of y-direction which is observed in thermal Eq. (3) for the term $\frac{1}{(\rho c)_f}\frac{\partial q_r}{\partial y}$. By using the Ross eland's approximations, the radiative heat flux q_r taken from the previous study by Roja *et al.,* [39], Nagaraja *et al.,* [40] is stated as

$$q_r = -\frac{4\sigma^*}{3k^*}\frac{\partial T^4}{\partial y} \tag{5}$$

Here, q_r is radiation term, k^* signifies the coefficient of mean absorption and σ^* signifies the Stefan-Boltzmann constant. Since there is slight temperature variation inside the flow the term T^4 has been taken about T_∞, using Taylor's series expansion and neglecting higher powers, we have

$$T^4 \cong 4({T_\infty}^3)T - 3({T_\infty}^4) \tag{6}$$

By incorporating Eq. (6) in Eq. (5), we write the term

$$\frac{\partial q_r}{\partial y} = -\frac{4\sigma^* {T_\infty}^3}{3k^*}\frac{\partial^2 T}{\partial y^2} \tag{7}$$

Utilizing Eq. (7) in Eq. (3) which reduces to

$$u\frac{\partial T}{\partial x} + v\frac{\partial T}{\partial y} = \left(\alpha^* + \frac{16\sigma^* {T_\infty}^3}{3k^*(\rho c)_f}\right)\frac{\partial^2 T}{\partial y^2} + \tau\left[D_B\frac{\partial C}{\partial y}\frac{\partial T}{\partial y} + \frac{D_T}{T_\infty}\left(\frac{\partial T}{\partial y}\right)^2\right] + \frac{Q}{(\rho c)_f}(T - T_\infty) \tag{8}$$

With the boundary conditions given by Biswal *et al.,* [23]:

$$\left.\begin{array}{c} v = v_w, u = u_w(x),\ -k\frac{\partial T}{\partial y} = h_f(x)(T_w - T),\ C_w = C_\infty + bx\ at\ y = 0 \\ u \to 0, T \to T_\infty, C \to C_\infty, as\ y \to \infty \end{array}\right\} \quad (9)$$

Where, $\alpha^* = \frac{k}{(\rho c)_f}$ denotes thermal diffusivity (m^2s^{-1}), k denotes thermal conductivity (W m^{-1} K^{-1}), $\vartheta = \frac{\mu}{\rho_f}$ represents kinematic viscosity ($m^2 s^{-1}$), μ is dynamic viscosity (Ns/ m^2), ρ_f is the density of the fluid (kg m^{-3}), C_p denotes heat capacity (J Kg^{-1} K^{-1}), σ is denoted as electrical conductivity (sm^{-1}), $\beta = \mu_B \frac{\sqrt{2\pi_c}}{P_y}$ represents Casson fluid parameter, Q is heat generation coefficient, h_f represents heat transfer coefficient, the expression $\tau = \frac{(\rho c)_p}{(\rho c)_f}$ represents ratio of $(\rho c)_p$ thermal capacity of nano-sized particles (Kg/ m^3 K) to the $(\rho c)_f$ thermal capacity of the base (J/ m^3 K). β_T represents coefficient of thermal expansion (1/K), β_C represents coefficient of mass expansion of the fluid, D_B and D_T are denoted as coefficients of Brownian motion and thermophoresis respectively, K_0 is the coefficient of the chemical reaction and u denotes velocity along x -direction and v represents the velocity along y -direction is defined as;

$$u = \frac{\partial \psi}{\partial y}\ and\ v = -\frac{\partial \psi}{\partial x}$$

Where, $\psi = \sqrt{a\vartheta}xf(\eta)$ denotes the stream function and $\eta = \sqrt{\frac{a}{\vartheta}}y$, denotes similarity variable.

To simplify the mathematical analysis, we introduce the following similarity transformations:

$$\left.\begin{array}{l} u = axf'(\eta)\ and\ v = -\sqrt{a\vartheta}f(\eta) \\ \theta(\eta) = \frac{T-T_\infty}{T_w-T_\infty}\ and\ \emptyset(\eta) = \frac{C-C_\infty}{C_w-C_\infty} \end{array}\right\} \quad (10)$$

The governing Eq. (1) - Eq. (2), Eq. (4) and Eq. (8) are reduced into ordinary differential equations using similarity transformations from Eq. (10) as follows:

$$\left(1 + \frac{1}{\beta}\right)f''' - f'^2 + ff'' + G_r\theta\cos\alpha + G_c\emptyset\cos\alpha - Mf' - Kf' = 0 \quad (11)$$

$$\frac{1}{Pr}\left(1 + \frac{4}{3}R\right)\theta'' + f\theta' + Nb\theta'\emptyset' + Nt\theta'^2 + \lambda\theta = 0 \quad (12)$$

$$\emptyset'' + Lef\emptyset' + \frac{Nt}{Nb}\theta'' - LeS\emptyset = 0 \quad (13)$$

The boundary conditions Eq. (9) are reduced to:

$$\left.\begin{array}{c} f(\eta) = f_w, f'(\eta) = 1, \theta'(\eta) = -Bi\left(1 - \theta(\eta)\right),\ \emptyset(\eta) = 1\ at\ \eta = 0 \\ f'(\eta) \to 0,\ \theta(\eta) \to 0,\ \emptyset(\eta) \to 0, as\ \eta \to \infty \end{array}\right\} \quad (14)$$

The non-dimensional parameters which are obtained in Eq. (11) through Eq. (14) are, $f'(\eta)$ represents velocity profile, $\theta(\eta)$ represents temperature profile, and $\emptyset(\eta)$ represents the concentration profile. Governing parameters are $f_w = -\frac{v_w}{\sqrt{a\vartheta}}$, denote Suction parameter, $M = \frac{\sigma {B_o}^2}{a\rho_f}$, denote Magnetic parameter, $K = \frac{\vartheta}{aK^{**}}$, represent porosity parameter, $G_r = \frac{g\beta_T(T_W - T_\infty)}{a^2 x}$ represents Grashof number, $G_c = \frac{g\beta_c(C_W - C_\infty)}{a^2 x}$ modified Grashof number, Bi represents Biot number, $Nt = \frac{(\rho c)_p D_T(T_W - T_\infty)}{(\rho c)_f \vartheta T_\infty}$ Thermophoresis parameter, $Nb = \frac{(\rho c)_p D_B(C_W - C_\infty)}{(\rho c)_f \vartheta}$ Brownian motion parameter, $Pr = \frac{\vartheta}{\alpha^*}$ Prandtl number, $R = \frac{4\sigma^* T_\infty^3}{k^* k}$, Radiation parameter, $Le = \frac{\vartheta}{D_B}$, Lewis number, $\lambda = \frac{Q}{a(\rho c_p)_f}$ denote Heat Generation, and $S = \frac{K_o}{a}$, Chemical reaction parameter.

The subsequent equations provided below are utilized to determine the local skin friction, local Nusselt number, and local Sherwood numbers:

$$C_f = \frac{\tau_w}{\rho u_w^2},\ Nu = \frac{x q_w}{k(T_W - T_\infty)},\ Sh = \frac{x h_m}{D_B(C_W - C_\infty)} \tag{15}$$

$$\tau_w = \rho\vartheta\left(u_y\right)_{y=0}, q_w = -k\left(T_y\right)_{y=0}, h_m = -D_B\left(\emptyset_y\right)_{y=0} \tag{16}$$

By using the above equations, we have

$$C_f\sqrt{Re} = f''(0), \frac{Nu}{\sqrt{Re}} = -\theta'(0), \frac{Sh}{\sqrt{Re}} = -\emptyset'(0) \tag{17}$$

Where, Re, Nu, Sh and C_f represent the Reynolds number, Nusselt number, Sherwood number and skin friction, respectively.

3. Numerical Analysis

The nonlinear Eq. (11) through Eq. (13) are resolved using the 4th-order Runge-Kutta method in conjunction with the shooting technique with appropriate boundary conditions Eq. (14), here are equations expressed as taken from a previous study by Koka R *et al.,* [32]. Figure 2 shows Flow Chart for 4th-order Runge-Kutta method with shooting technique

$$f''' = \frac{(-ff'' + f'^2 - G_r\theta\cos\alpha - G_c\emptyset\cos\alpha + Mf' + Kf')}{\left(1 + \frac{1}{\beta}\right)} \tag{18}$$

$$\theta'' = -Pr\frac{(f\theta' + \mathrm{Nb}\emptyset'\theta' + \mathrm{Nt}\theta'^2 + \theta\lambda)}{(1 + \frac{4}{3}R)} \tag{19}$$

$$\emptyset'' = -Lef\emptyset' - \frac{\mathrm{Nt}}{\mathrm{Nb}}\theta'' + LeS\emptyset \tag{20}$$

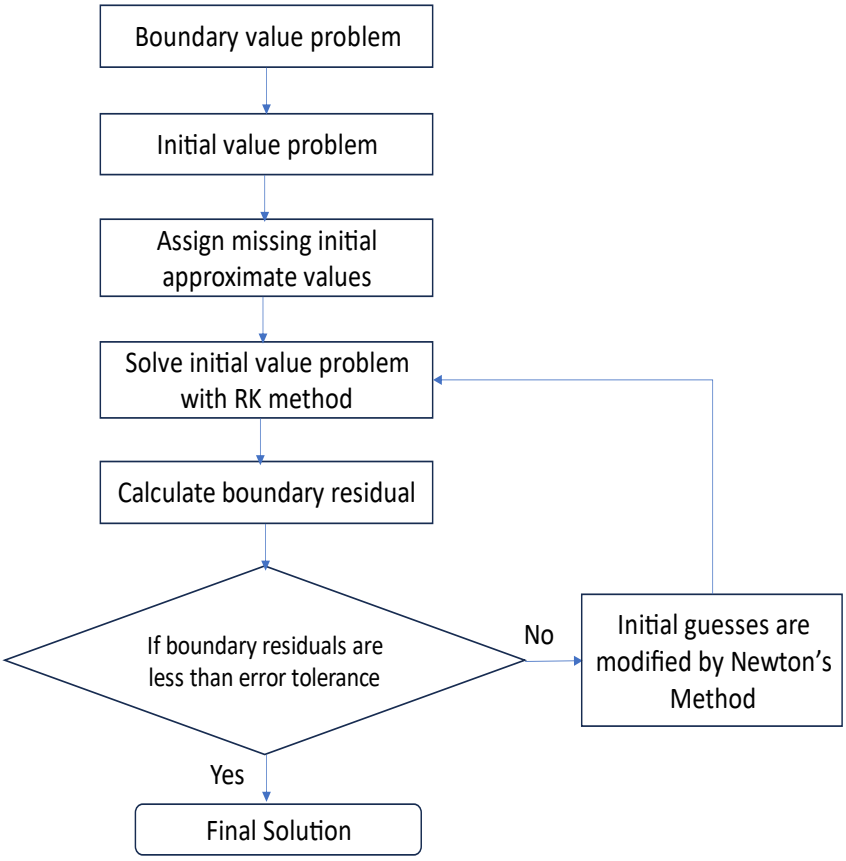

Fig. 2. Flow Chart for 4th-order Runge-Kutta method with shooting technique

The shooting technique transforms the boundary value problem associated with an ordinary differential equation (ODE) into the corresponding initial value problem for the purpose of facilitating their solution.

we now proceed by introducing new variables in the following manner:

$$f_1 = f;\ f_2 = f';\ f_3 = f'';\ f_4 = \theta;\ f_5 = \theta';\ f_6 = \emptyset;\ f_7 = \emptyset' \tag{21}$$

From higher order nonlinear coupled differential equations and corresponding boundary conditions are derived from seven equations first ordered differential equations are formulated, along with corresponding boundary conditions. These differential equations are as follows:

$$\left.\begin{aligned} f_1' &= f_2 \\ f_2' &= f_3 \\ f_3' &= \frac{(-f_1 f_3 + f_2^2 - G_r\theta\cos\alpha - G_c\emptyset\cos\alpha + Mf_2 + Kf_2)}{\left(1+\frac{1}{\beta}\right)} \\ f_4' &= f_5 \\ f_5' &= \Pr\frac{(-f_1 f_5 - Nbf_5 f_7 - Ntf_5^2 - \lambda f_4)}{(1+\frac{4}{3}R)} \\ f_6' &= f_7 \\ f_7' &= -Lef_1 f_7 + \frac{Nt}{Nb}\Pr\frac{(-f_1 f_5 - Nbf_5 f_7 - Ntf_5^2 - \lambda f_4)}{\left(1+\frac{4}{3}R\right)} + SLef_6 \end{aligned}\right\} \tag{22}$$

With the boundary conditions as:

$$\left.\begin{matrix} f_1(0) = f_w,\ f_2(0) = 1, f_5(0) = -Bi(1 - f_4(0));\ f_6(0) = 1, \\ f_2(\infty) = 0,\ \ f_4(\infty) = 0, f_6(\infty) = 0 \end{matrix}\right\} \tag{23}$$

For the effective application of the RK-4 (Runge-Kutta) method, a finite domain of $0 \leq \eta \leq \infty$ is essential. The exact values of relevant parameters determine the appropriate value for the present model. The RK technique and the shooting method are used to solve the set of ordinary differential equations that occurs when the convergence criterion is satisfied in this case, $\eta_\infty \leq 10$. This numerical method has the advantage of handling intricate equation systems and providing insights into fluid flow behaviour that may be challenging to get using analytical methods. This technique helps get the intended result within the constraints. Subsequently, the entire procedure is iterated until the predetermined target outcomes are set at 10^{-6}.

4. Results and Discussion

Analysing the movement of a steady, laminar, incompressible Casson nanofluid over an inclined stretching sheet in the presence of a magnetic field while accounting for radiative, heat generation, and chemical reaction effects is the focus of current research. The ordinary differential equations (ODEs) resulting from the nonlinear flow simulation are then analytically analysed by means of the Runge-Kutta 4th order with a shooting approach. Parametric analysis was carried out for a physical comprehension of matter, and the geometric findings that were made are shown graphically. The mathematical model for the profiles of velocity, temperature, and concentration is found for various parametric values.

Recent findings were compared with published literature to verify their veracity. Table 1 summarises the current study's findings, which are in line with observations for local Sherwood and local Nusselt numbers with Nt thermophoresis parameter and Nb Brownian motion parameter for $Le = Pr = 10$ made by Noghrehabadi *et al.,* [35] and Barik *et al.,* [24].

Table 1
Comparison results for local Sherwood and Nusselt numbers for $Pr = Le = 10$

		Noghrehabadi *et al.,* [35]	Barik *et al.,* [24]	Current finding	Noghrehabadi *et al.,* [35]	Barik *et al.,* [24]	Current finding
Nt	Nb	$-\theta'(0)$	$-\theta'(0)$	$-\theta'(0)$	$-\emptyset'(0)$	$-\emptyset'(0)$	$-\emptyset'(0)$
0.1	0.1	0.9523768	0.9526	0.9529437	2.1293938	2.131	2.1359134
0.2	0.1	0.6931743	0.6932	0.6932690	2.2740215	2.277	2.2737061
0.3	0.1	0.5200790	0.5200	0.5205826	2.5286382	2.532	2.5284642
0.4	0.1	0.4025808	0.4024	0.4021643	2.7951701	2.799	2.7962418
0.5	0.1	0.3210543	0.3209	0.3214390	3.0351425	3.040	3.0341927
0.1	0.2	0.5055814	0.5053	0.5055867	2.3818706	2.384	2.3807152
0.1	0.3	0.2521560	0.2517	0.2528614	2.4100188	2.412	2.4164159
0.1	0.4	0.1194059	0.1189	0.1181128	2.3996502	2.402	2.4100129
0.1	0.5	0.0542534	0.0539	0.0553448	2.3835712	2.385	2.3902903

Table 2
Results for different dimensionless parameter values pertaining to local skin friction, Local Nusselt number, and Local Sherwood number

β	M	Pr	K	Le	λ	R	S	$f''(0)$	$-\theta'(0)$	$-\emptyset'(0)$
0								−0.1666712	0.8504946	3.0552525
0.5								−0.9497971	0.8224030	3.0124734
1								−1.2052061	0.8153489	2.9996662
	0							−0.6814861	0.8311206	2.0264579
	0.5							−0.7703924	0.8281526	2.0217955
	1							−0.84979702	0.8255752	2.0355999
		0.71						−0.46777287	0.8391137	2.0381876
		3						−0.47522373	0.9392045	2.0128781
		7.5						−0.47630447	0.9674525	1.9995890
			0					−0.41602855	0.8409829	1.0264579
			0.5					−0.46777288	0.8391137	1.0217955
			1					−0.51514115	0.8373968	1.0176837
				10				−0.46777288	0.8391137	1.0217955
				20				−0.47006312	0.8390186	2.1310723
				30				−0.47091202	0.8389856	3.1699871
					0.1			−0.46777288	0.0839113	2.0381876
					0.3			−0.46581806	0.0816243	2.0432004
					0.5			−0.46249072	0.0778361	2.0511891
						4		−0.45686253	0.0737620	2.0551602
						6		−0.45348427	0.0709024	2.0598759
						8		−0.45140009	0.0691776	2.0627694
							0.3	−0.46777288	0.0839113	2.0381876
							0.5	−0.46784894	0.0839110	2.1984586
							1	−0.46801611	0.0839102	2.5811289

Figure 3 demonstrates $f'(\eta)$ velocity profile decreases as values of β Casson fluid parameter increase. The Casson fluid exhibits significant variations in plastic dynamic viscosity as β increases, which in turn significantly affects yield stress.

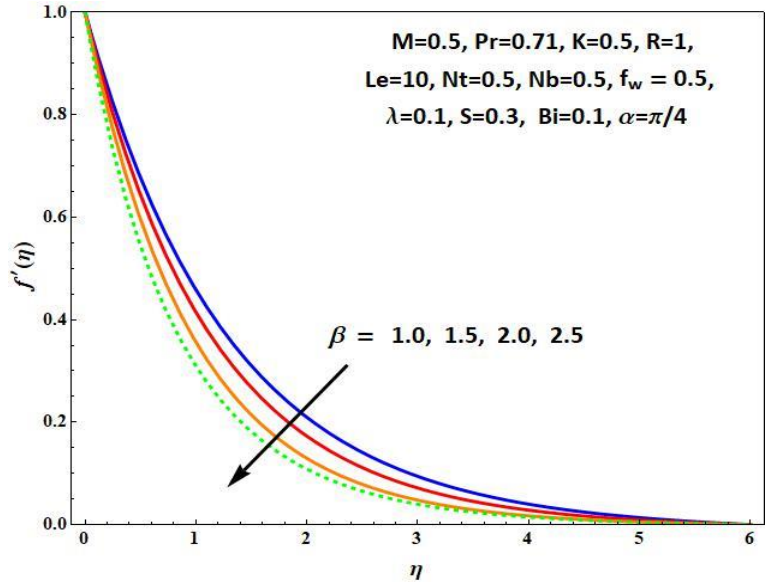

Fig. 3. Effects of β on velocity profile $f'(\eta)$ for $f_w = 0.5, Pr = 0.71, Le = 10,\ Nt = Nb = 0.5$ values

The temperature within the boundary layer $\theta(\eta)$ improvised by a change in the Casson fluid parameter β in Figure 4, which results in a drop in yield stress. Physically, this happened due to interactions and enhanced molecular mobility, which rise β values and ultimately increase the pace at which fluid temperature rises. The temperature boundary layer thickens as a result. The influence of α inclined angle on the velocity profiles are shown in Figure 5.

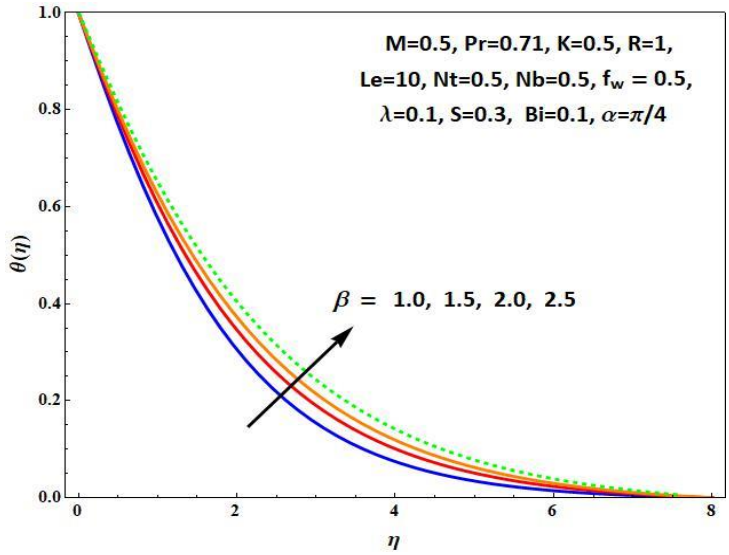

Fig. 4. Effects of β on temperature profile $\theta(\eta)$ for $f_w = 0.5, Pr = 0.71, Le = 10,\ Nt = Nb = 0.5$ values

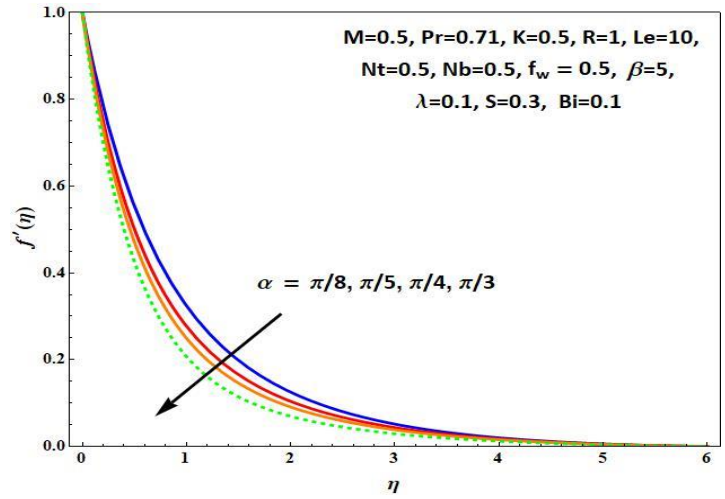

Fig. 5. Effects of α on velocity profile $f'(\eta)$ for $f_w = 0.5, Pr = 0.71, Le = 10, Nt = Nb = 0.5$ values

The influence of α inclined angle on the temperature and velocity profiles are shown in Figure 6 and Figure 7. It shows that an increase in α improves $\theta(\eta)$ temperature profile, it also slows down fluid velocity and reduces $f'(\eta)$ velocity profile. This phenomenon occurs because of a greater inclination angle, which lowers buoyancy forces and raises fluid temperature by lowering fluid velocity taken from a previous study by Biswal *et al.,* [23].

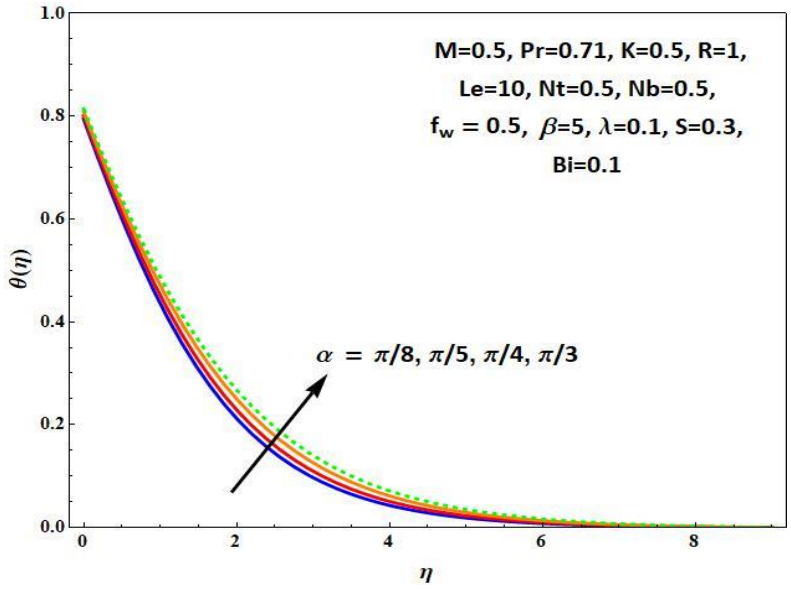

Fig. 6. Effects of α on temperature profile $\theta(\eta)$ for $f_w = 0.5, Pr = 0.71, Le = 1, Nt = Nb = 0.5$ values

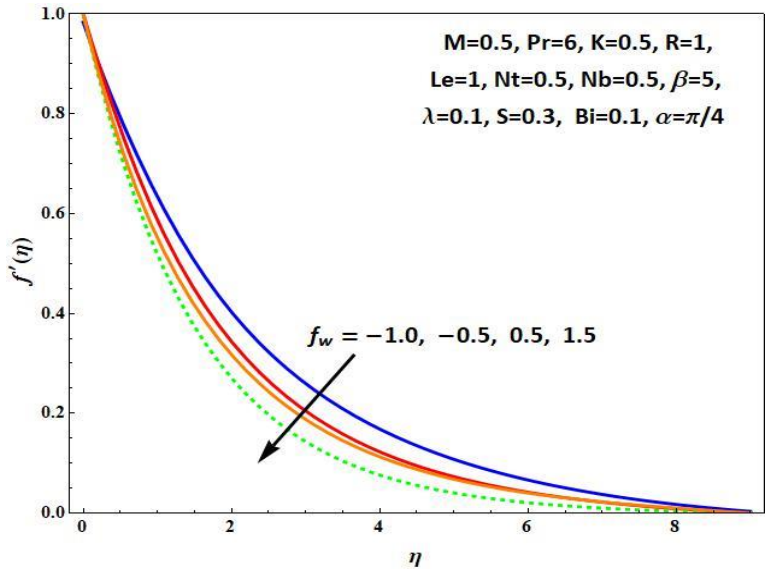

Fig. 7. Effects of f_w on velocity profile $f'(\eta)$ for $Pr = 6, Le = 1, Nt = Nb = 0.5, \beta = 5$ values

Figure 7 illustrates how the f_w suction/injection parameter affects $f'(\eta)$ velocity profile and the thickness of the velocity boundary layer that causes the velocity to slow down. Furthermore, because of yield stress, a rise in fluid viscosity seems to reduce velocity boundary layer thickness. An f_w suction/injection parameter increases, a corresponding rise in the $\theta(\eta)$ temperature profile within thermal boundary layer is depicted in Figure 8. This implies temperature distribution is positively impacted by a rise in the suction parameter.

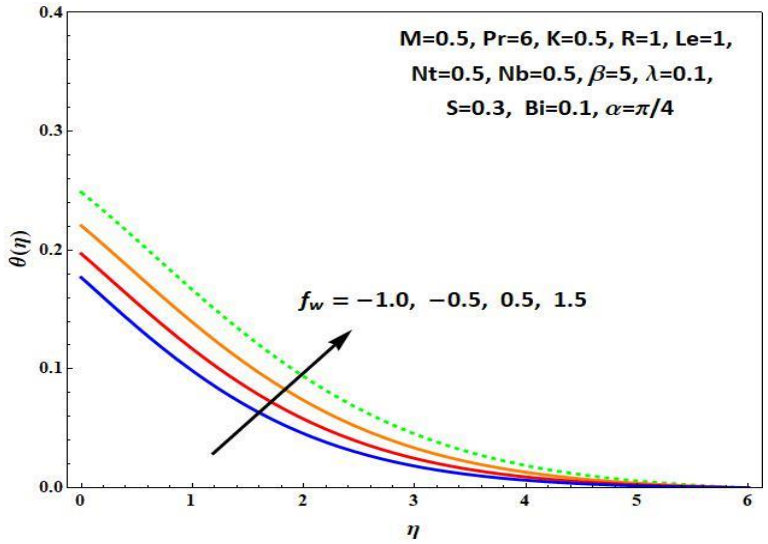

Fig. 8. Variation of f_w on temperature profile $\theta(\eta)$ for $Pr = 0.71, Le = 10, Nt = Nb = 0.5, \beta = 5$ values

Figure 9 represents the influence of M magnetic parameter on $f'(\eta)$ velocity profile. An increasing M results in a reduced dimensionless velocity field. This phenomenon occurs because as electromagnetic force strengthens, it impedes the movement of fluid particles, leading to a decrease in the velocity field taken from a previous study by Alhadhrami *et al.,* [56].

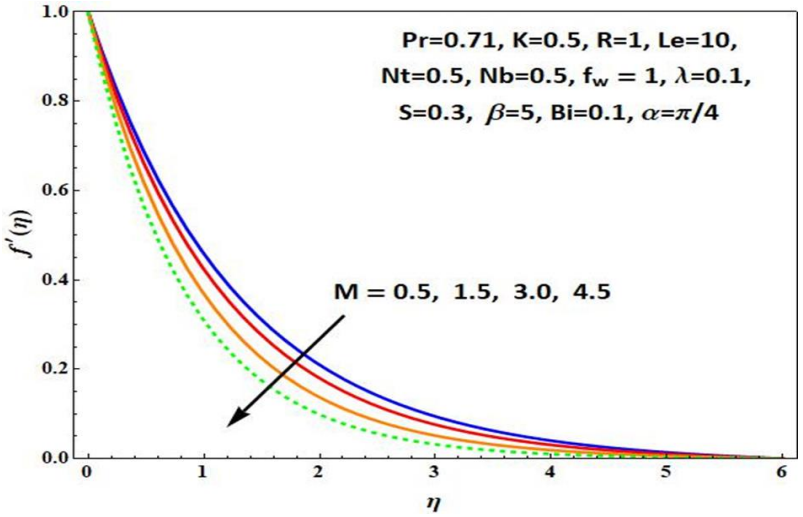

Fig. 9. Variation of M on velocity profile $f'^{(\eta)}$ for $Pr = 0.71, Le = 10, Nt = Nb\ 0.5, \beta = 5$ values

Figure 10 displays the impacts of Mmagnetic parameter on $\theta(\eta)$ temperature profile, showing that the values of M increase, the thermal layer's thickness also grows. Elevated magnetic parameter values correspond to a greater resistive Lorentz force, which amplifies the kinetic energy generated by diffusion processes. Consequently, the temperature field experiences warming.

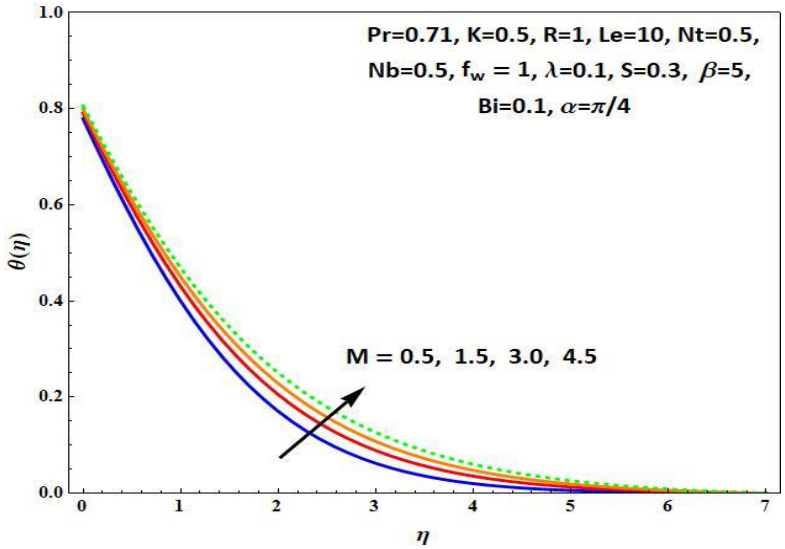

Fig. 10. Variation of M on temperature profile $\theta(\eta)$ for $Pr = 0.71, Le = 10, Nt = Nb = 0.5, \beta = 0.5$ values

Figure 11 shows the velocity profile $f'(\eta)$ across various values of porosity parameter K, with keeping all other factors constant. It is found that higher values of K associated with enhanced velocity and a thicker boundary layer. This phenomenon demonstrates that as K values rise, resistance within porous media diminishes, which, in turn, supports the acceleration of the flow regime's momentum and consequently improves the velocity field. K porosity parameter is stimulated on $\theta(\eta)$ temperature profile as depicted in Figure 12. As K increases, there is a corresponding increase in the temperature of the fluid. The liquid's viscosity increases with an increase in K, and as a result, its velocity decreases as it travels past surfaces with higher regulation. This supports the hypothesis from a prior work by Alhadhrami *et al.,* [56] that greater stress is created as K increases, thickening the thermal boundary layer.

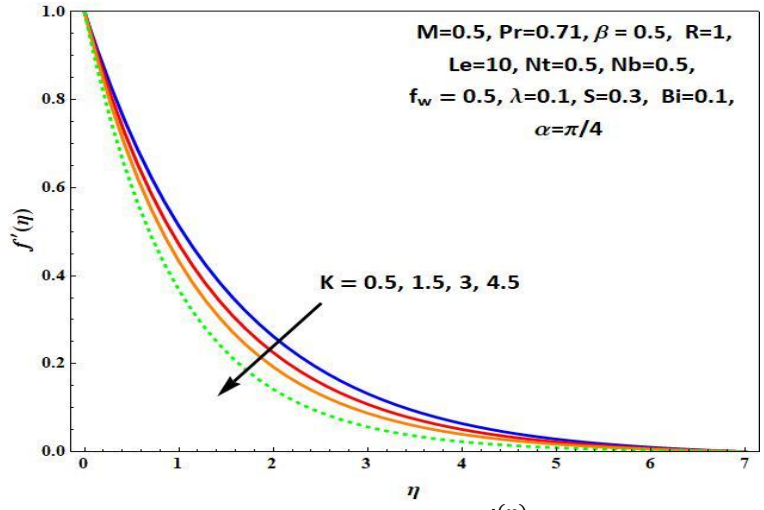

Fig. 11. Effects of K on velocity profile $f'^{(\eta)}$ for $Pr = 10, Le = 10, Nt = Nb = 0.5,\ \beta = 0.5$ values

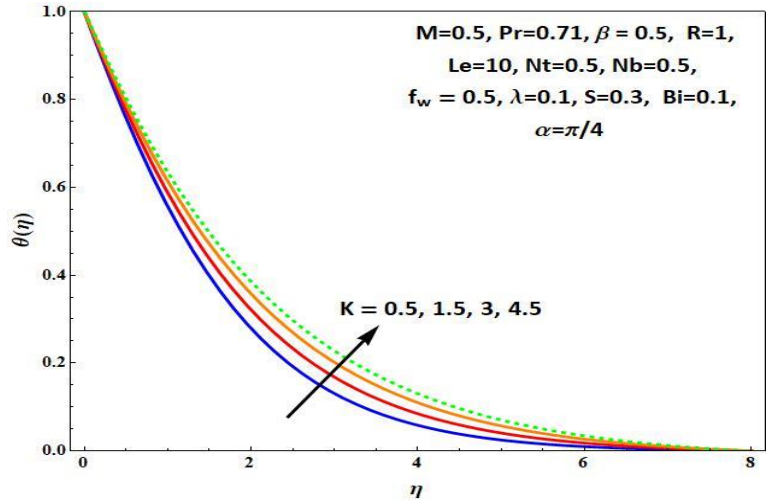

Fig. 12. Effects of K on temperature profile $\theta(\eta)$ for $Pr = 0.71, Le = 10, Nt = Nb = 0.5, \beta = 0.5$ values

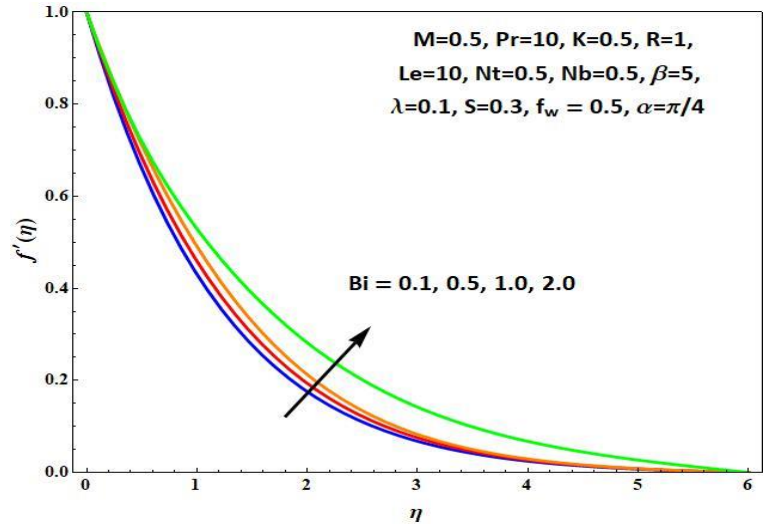

Fig. 13. Effects of Bi on velocity profile $f'(\eta)$ for $Pr = 10, Le = 10$ values

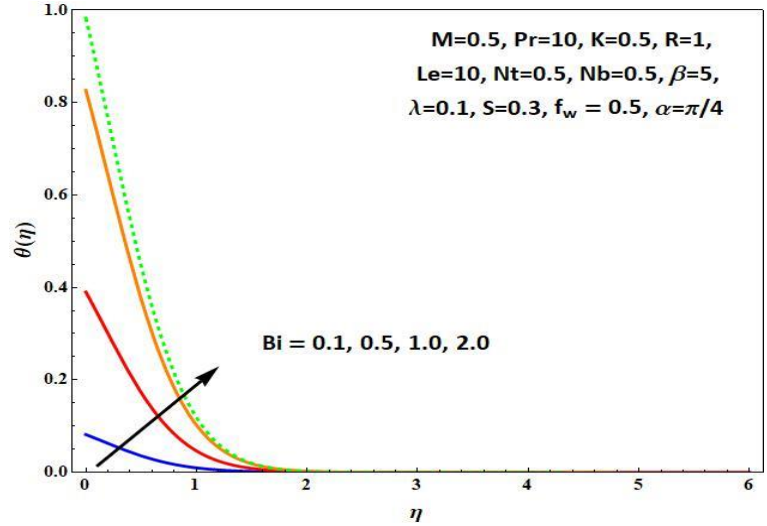

Fig. 14. Effects of Bi on temperature profile $\theta(\eta)$ for $Pr = 10, Le = 10$ values

Figure 13 reveals that an increment in Bi Biot number increases the velocity profile $f'(\eta)$. When $Bi > 0$, it indicates that convective heat transfer prevails at the surface, defining Newtonian cooling processes where the heat transfer rate is directly linked with the temperature difference between the surfaces and surrounding fluid, potentially causing an increase in fluid velocity. Figure 14 shows the temperature distribution for $Bi > 0$. Heat transfers from the solid surface to the fluid, and thus, an increase in Bi Biot number results in elevated temperature within the fluid layer. Additionally, it is noted that when the Bi Biot number is high; the surface temperature is significantly low owing to the low conductivity of the solid surface results observed by Biswal *et al.,* [23].

The impact of the G_r Grashof number can be observed in Figure 15 & Figure 16, which display velocity $f'(\eta)$ and $\theta(\eta)$ temperature profiles obtained from numerical simulations for different Grashof number values. As the Grashof number increases, buoyancy forces intensify accelerating the flow. Consequently, within boundary layer, the velocity rises, as depicted in Figure 15. On the contrary, due to the cooling surface assumption, the temperature profile diminishes with increasing G_r Grashof numbers as shown in Figure 16. This outcome results in a thinner thermal boundary layer, aligning with expectations taken from a previous study by Yusof Zanariah *et al.,* [58].

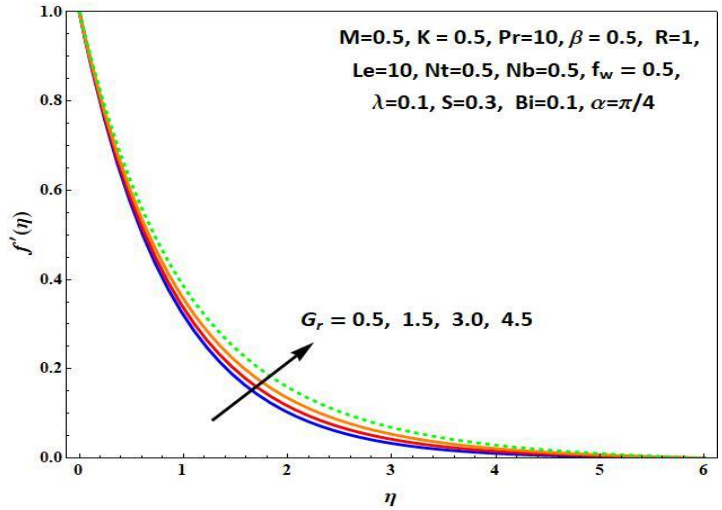

Fig. 15. Effects of G_r on velocity profile $f'(\eta)$ for $Pr = Le = 10$ values

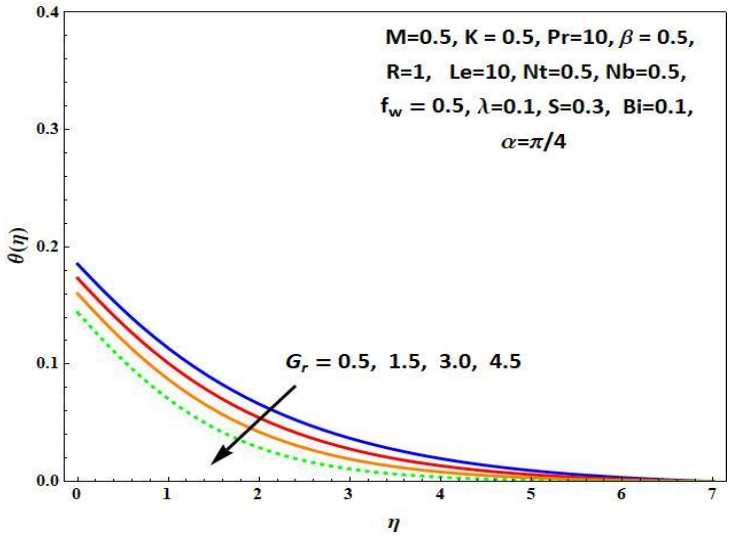

Fig. 16. Effects of G_r on temperature profile $\theta(\eta)$ for $Pr = Le = 10$ values

The impact of parameters in Figure 17, Figure 18, and Figure 19 depict thermophoresis Nt and Brownian motion Nb for various values of Pr and Le. The objective is to align the temperature profile $\theta(\eta)$ closely within the fluid's characteristics. The thickness of the thermal boundary layer indicates that the fluid's temperature increases with an increase Nb and Nt.

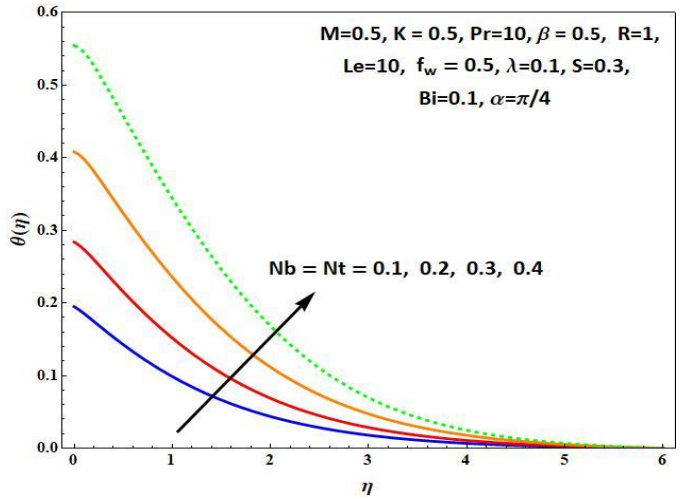

Fig. 17. Effects of Nt & Nb on temperature profile $\theta(\eta)$ for $Pr = Le = 10$ values

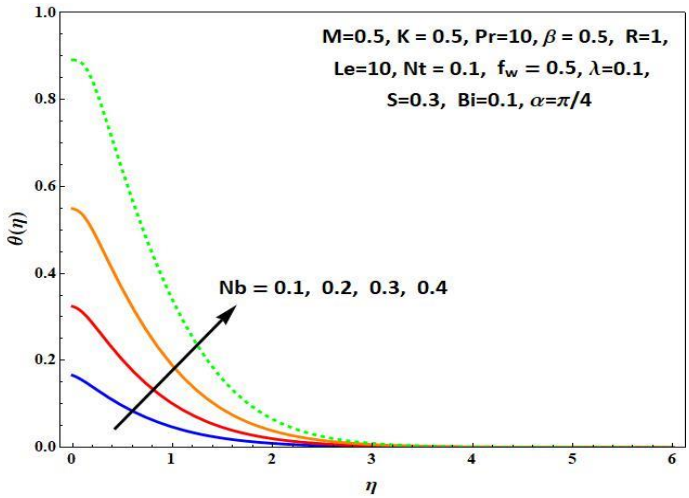

Fig. 18. Effects of Nb on temperature profile $\theta(\eta)$ for $Nt = 0.1, Pr = Le = 10$ values

The influence of $\theta(\eta)$ temperature profile for specific values of parameters Nt and Nb is affected by the Prandtl number Pr which correlates fluid's momentum transport and thermal transport properties, and the Lewis number Le associating the fluid's mass diffusion and thermal conductivity, as shown in Figure 20 and Figure 21. Consequently, decreasing $\theta(\eta)$ temperature profile and elevating the Pr and Le numbers leads to a decrease in the thickness of the boundary layer of the fluid. With a gradual rise in these parameters the temperature drops, enabling the fluid to discharge heat into the surrounding air.

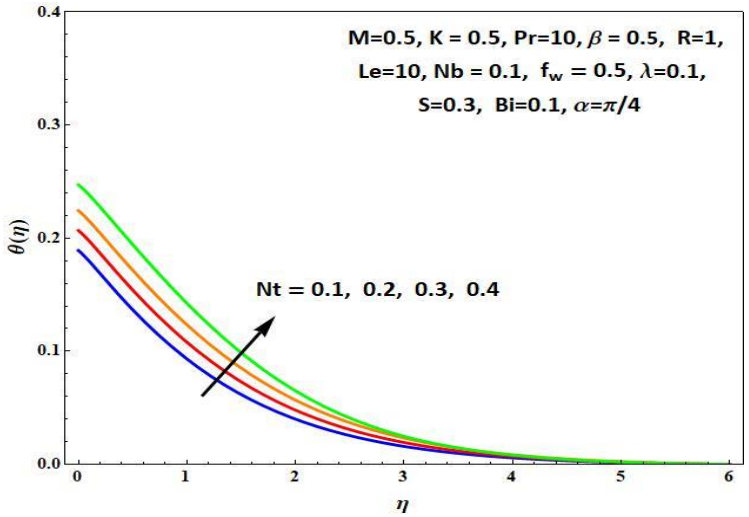

Fig. 19. Effects of Nt on temperature profile $\theta(\eta)$ for $Nb = 0.1, Pr = Le = 10$ values

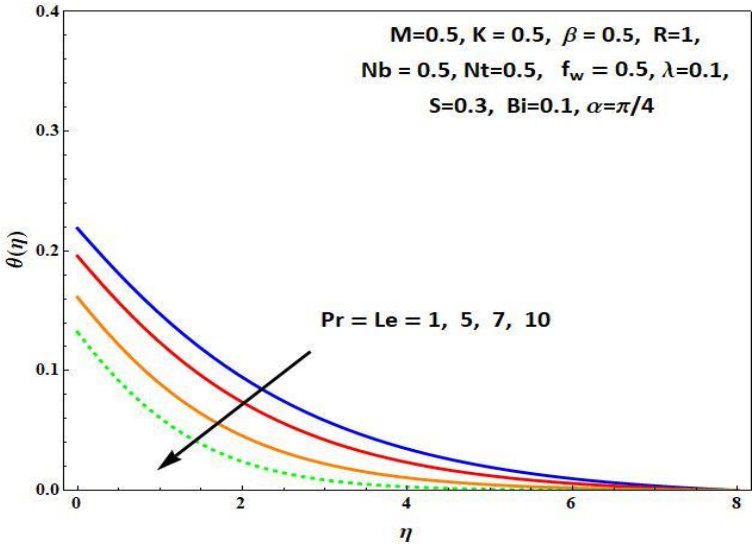

Fig. 20. Effects of Pr & Le on temperature profile $\theta(\eta)$ for $Nt = Nb = 0.5$ values

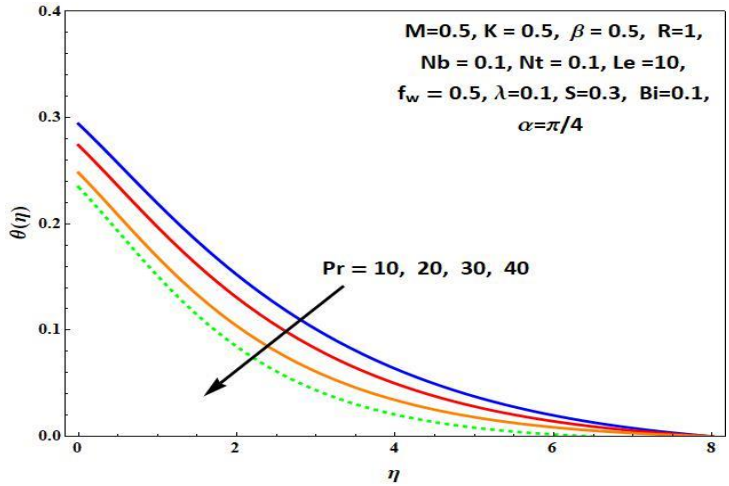

Fig. 21. Effects of Pr on temperature profile $\theta(\eta)$ for $Nt = Nb = 0.1, Le = 10$ values

Figure 22, Figure 23, and Figure 24 illustrate the impacts of Nb, Le, and Nt on concentration profile $\emptyset(\eta)$ of the chosen parameter values. These effects lead to an increased thickness of the concentration boundary layer for nanofluids. Contrary behaviour is noted in the boundary layer of nanofluid concentration regarding Brownian motion. It demonstrates that while the local Sherwood number exhibits a reversal trend, both coefficients exhibit an increase with higher volume percentages of nanoparticles. As Nb values rise, concentration consequently falls. The observation shows that as chosen parameter values increase, Nt will determine the increasing concentration of nanofluids.

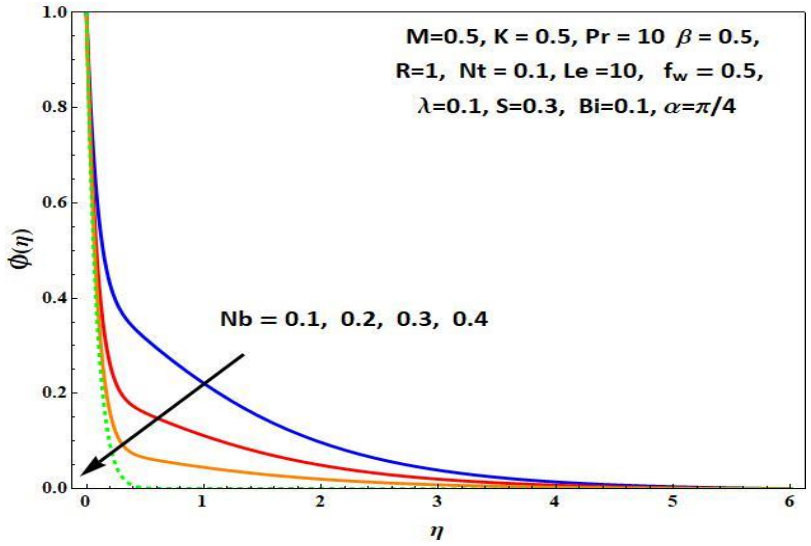

Fig. 22. Effects of Nb on concentration profile $\emptyset(\eta)$ for $Nt = 0.1, Le = Pr = 10$ values

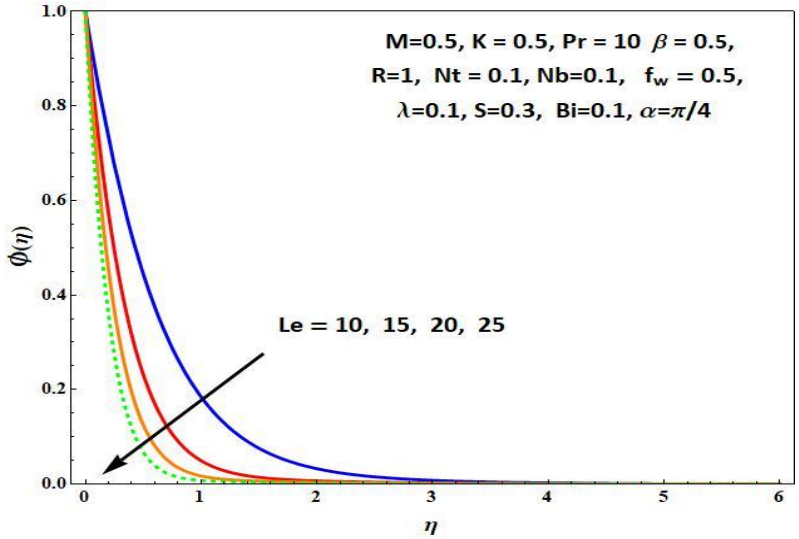

Fig. 23. Effects of Le on concentration profile $\emptyset(\eta)$ for $Nb = Nt = 0.1, Pr = 10$ values

For different values of the heat production parameter λ, Figure 25 displays $\theta(\eta)$ temperature distribution. In this case, λ is considered nonnegative. Results show that temperature distribution is minimised for small magnitudes of λ, but occurs at maximum temperature distribution $\theta(\eta)$for greater magnitude of λ. An event of heat production can physically heat the non-Newtonian Casson fluid inside thermal boundary layer.

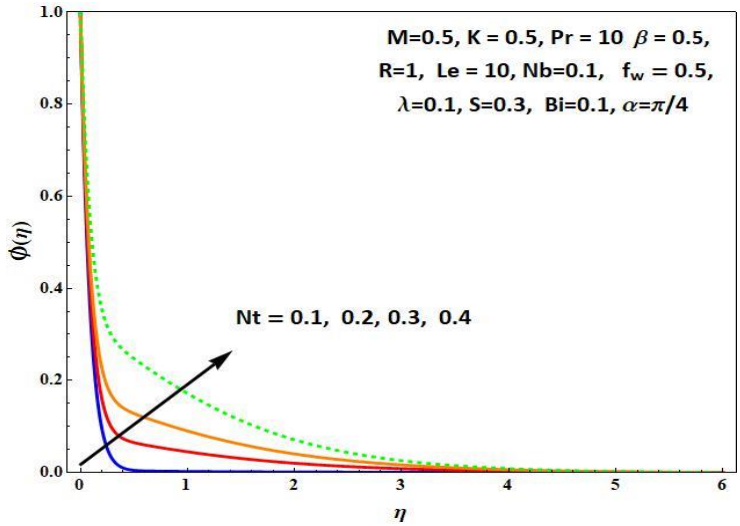

Fig. 24. Effects of Nt on concentration profile $\emptyset(\eta)$ for $Nb = 0.1, Pr = Le = 10$ values

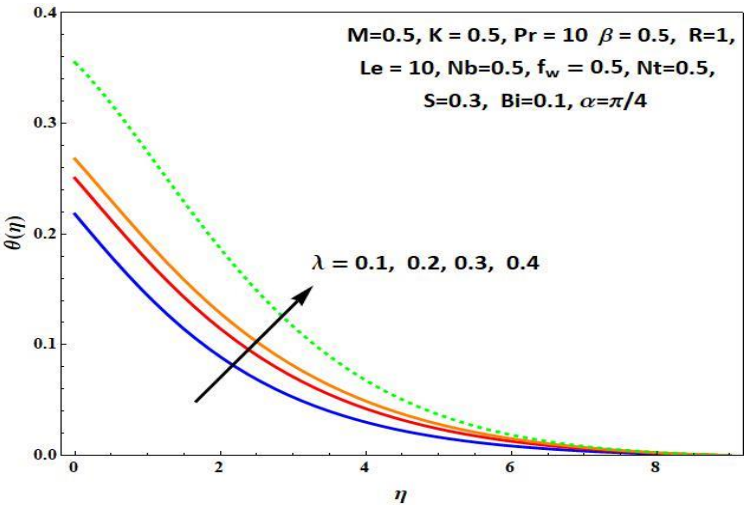

Fig. 25. Variation of λ on temperature profile $\theta(\eta)$ for $Nt = Nb = 0.5, Pr = Le = 10$ values

Figure 26 illustrates how a decrease in the heat source parameter λ increases mass diffusion while a rise in the value improves concentration diffusion. Hsiao *et al.,* [57] reported similar results in the literature.

The effects of chemical reaction parameter S on $\emptyset(\eta)$ concentration profile displayed in Figure 27. An increase in S signifies, leading to a reduction in the concentration profile $\emptyset(\eta)$. Elevated values of the chemical reaction parameter S are directly associated with a thinner concentration boundary layer, corroborated by earlier research conducted by Mummadisetty Umamaheswar *et al.,* [59].

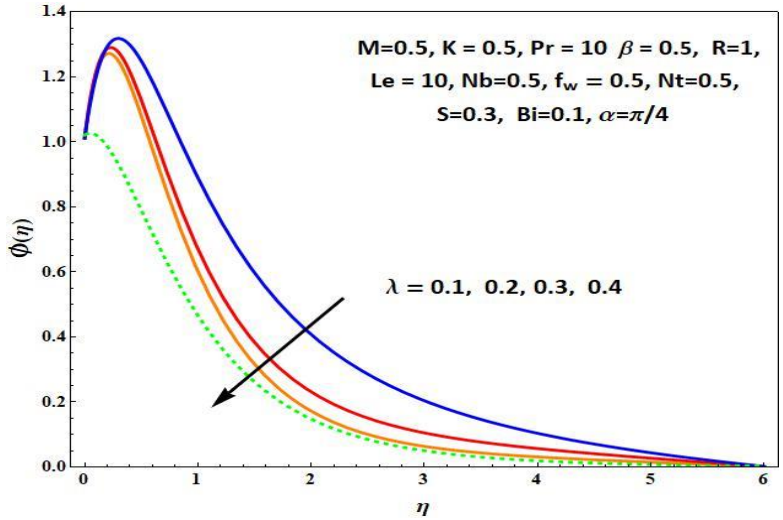

Fig. 26. Effects of λ on concentration profile $\emptyset(\eta)$ for $Nt = Nb = 0.5, Pr = Le = 10$ values

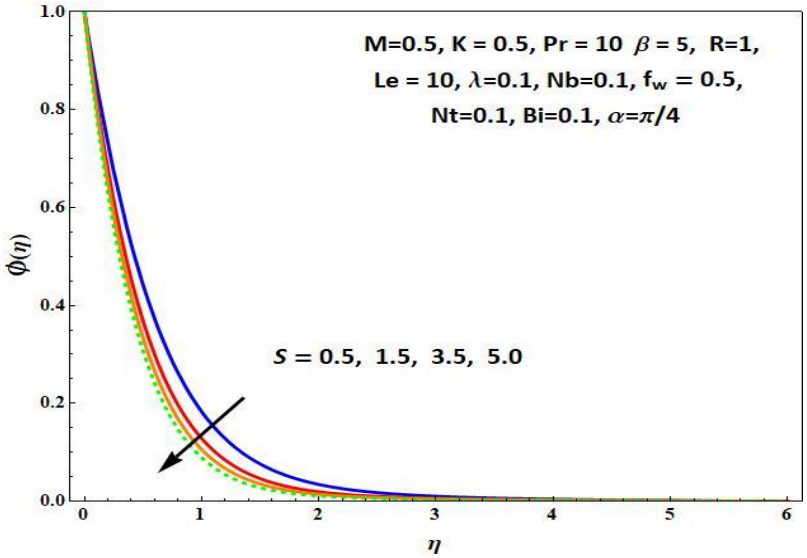

Fig. 27. Effects of S on concentration profile $\emptyset(\eta)$ for $Nt = Nb = 0.1, Pr = Le = 10$ values

The impact of R radiation parameter on $\theta(\eta)$ temperature profile as shown in Figure 28. The graph illustrates how fluid temperature increases as R increases, as observed in previous work by Barik *et al.,* [24]. This phenomenon arises from the decrease in the mean absorption coefficient k^* at larger values of R, causing a divergence in the radiative heat flux. Consequently, the radiation parameter persistently emits thermal energy into the flow zone, elevating the temperature of the nanofluid.

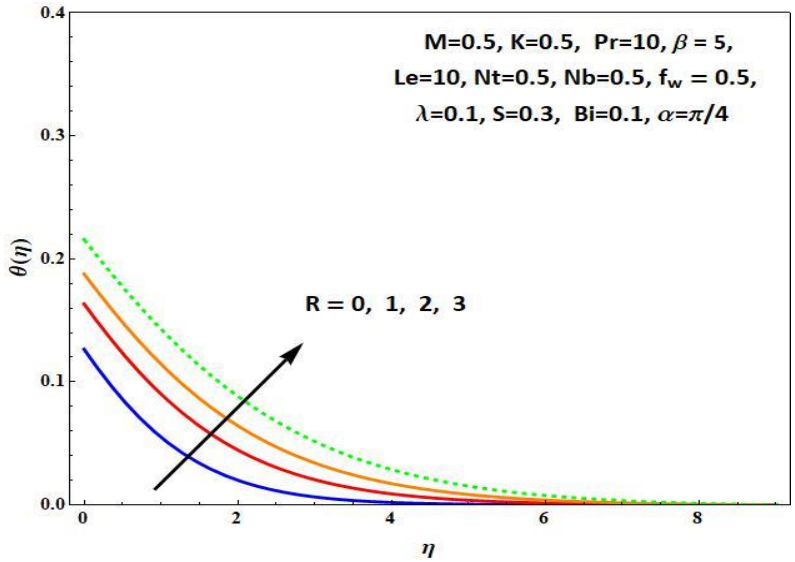

Fig. 28. Effects of R on temperature profile $\theta(\eta)$ for $Nt = Nb = 0.5, Pr = Le = 10$ values

Figure 29 depicts how the concentration profile $\emptyset(\eta)$ responds to changes in radiation parameter R. The graph indicates an increase in radiation parameter R leads to a decline in concentration rate, leading to thinning of species boundary layer observed by Barik *et al.,* [24]. Figure 30 and Figure 31 depict the impacts of Nb Brownian motion parameters on the rates of heat and concentration. As Brownian motion increases, the rate of heat reduction diminishes, while the concentration rate responds by increasing.

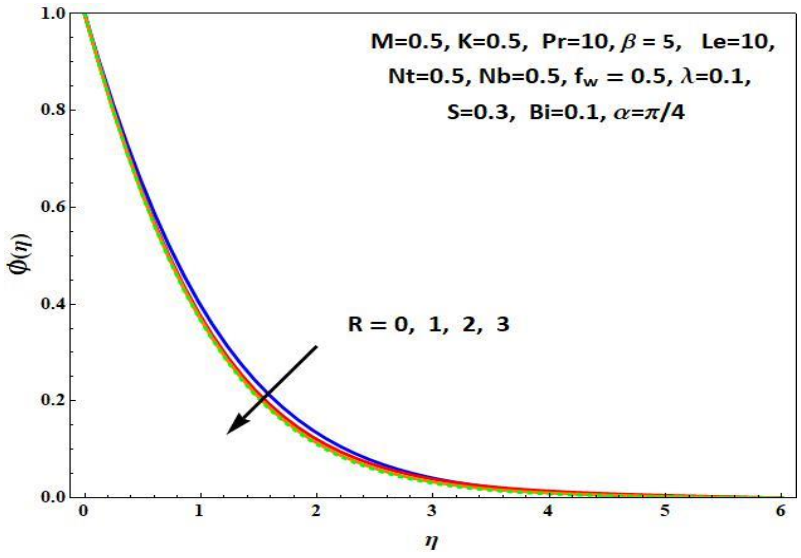

Fig. 29. Effects of R on concentration profile $\emptyset(\eta)$ for $Nt = Nb = 0.5, Pr = Le = 10$ values

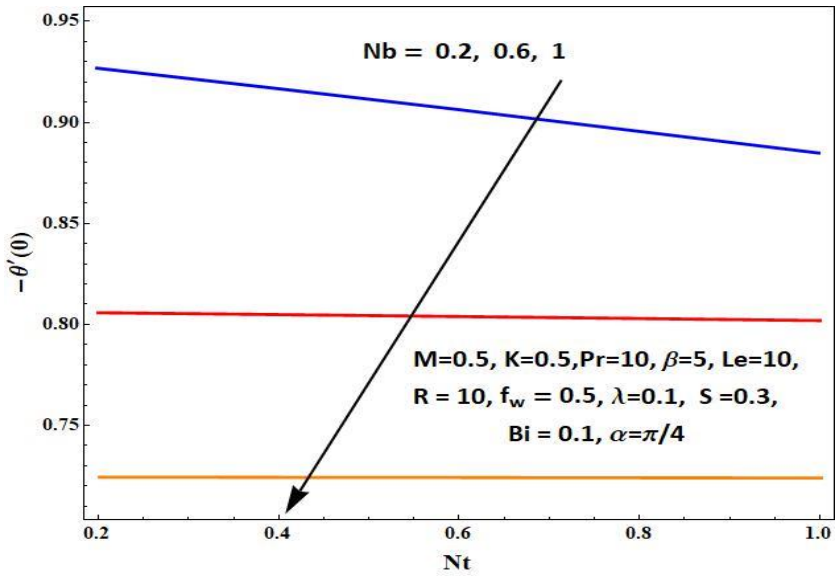

Fig. 30. Effects of Nb on Nusselt number for various Nt values

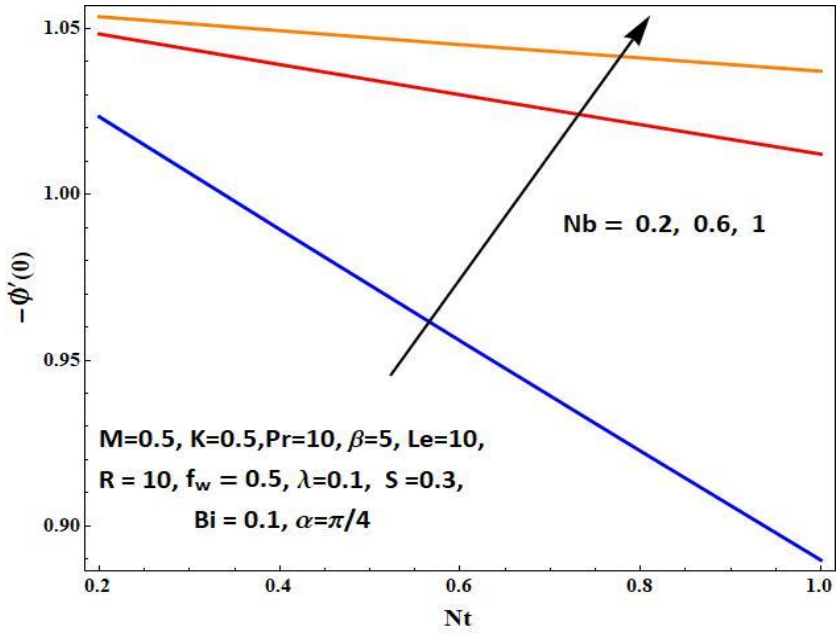

Fig. 31. Effects of Nb on Sherwood number for various Nt values

Heat transmission and concentration are influenced by the thermophoresis parameter Nt, as seen in Figure 32 and Figure 33. As thermophoresis intensifies, the rate of heat transfer diminishes, while the concentration rate exhibits an inverse trend.

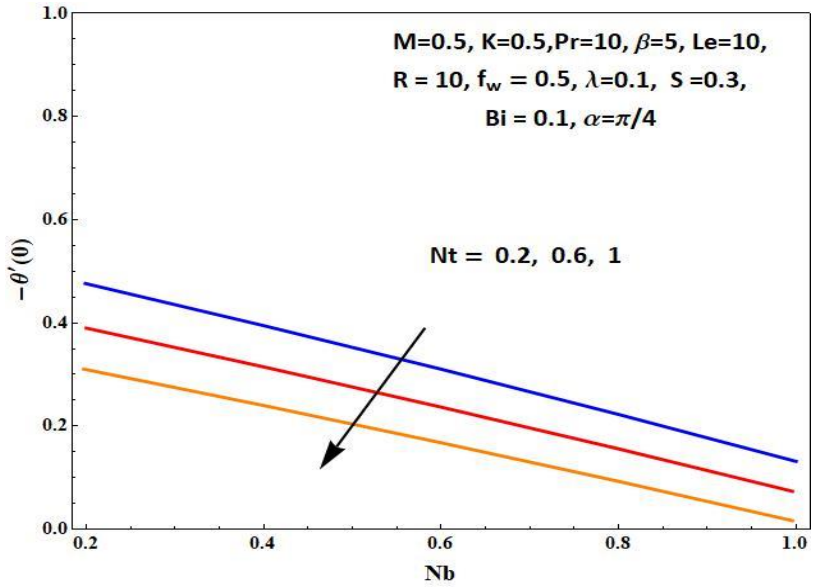

Fig. 32. Effects of Nt on Nusselt number for various Nb values

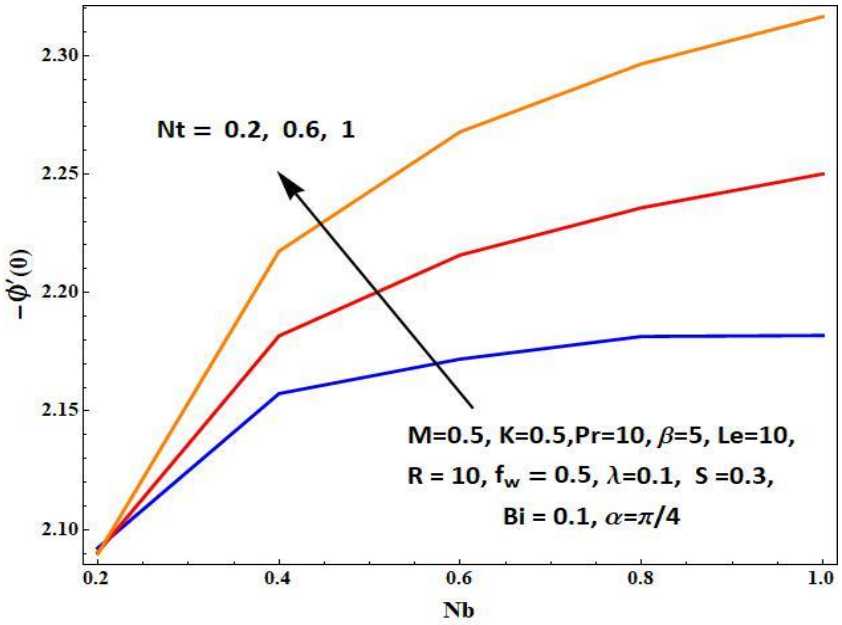

Fig. 33. Effects of Nt on Sherwood number for various Nb values

5. Conclusion

The research examines the impacts of heat generation, thermal radiation, and chemical reaction on the MHD flow of a Casson nanofluid across an inclined linearly stretched sheet within a homogeneous porous material, all while subjected to a magnetic field through numerical analysis. Graphical representations are utilized to demonstrate the effects of various crucial non dimensional parameters on temperature, concentration, and velocity profiles across a spectrum of physical conditions. When comparing our results to data that has been published, we found a significant level of agreement. The summary of key findings:

i. As β Casson parameter and M magnetic parameter values increase, there is a decrease in velocity. In contrast, both the concentration and heat transfer experience witness a concurrent rise.
ii. With an increase in porosity parameter K, a decline in the velocity profile is observed. Moreover, a higher K value leads to a significant thickening of the thermal boundary layer.
iii. The concentration profile $\emptyset(\eta)$ experiences evident enhancement with rising values of Prandtl number Pr, Lewis number Le.
iv. With increasing values of the angle of inclination α, which reduces buoyancy forces and elevates fluid temperature by decreasing fluid velocity.
v. An increasing Grashof number G_r effects the velocity and temperature profiles by regulating the balance between buoyancy and viscous forces as we observe enhanced temperature-reducing fluid motion.
vi. As the rate of heat generation parameter λ is enhanced, the temperature tends to rise while the concentration tends to decrease simultaneously.
vii. As R radiation parameter increases, both temperature and thermal boundary layer elevate, while concentration profile declines.
viii. Elevated chemical reaction parameter S results in an improved mass transfer rate.

Acknowledgement
This research was not funded by any grant.

Reference

[1] Choi, S. US, and Jeffrey A. Eastman. *Enhancing thermal conductivity of fluids with nanoparticles*. No. ANL/MSD/CP-84938; CONF-951135-29. Argonne National Lab.(ANL), Argonne, IL (United States), 1995.
[2] Gupta, Urvashi, Jyoti Sharma, and Mamta Devi. "Double-diffusive instability of Casson nanofluids with numerical investigations for blood-based fluid." *The European Physical Journal Special Topics* 230, no. 5 (2021): 1435-1445. http://dx.doi.org/10.1140/epjs/s11734-021-00053-9
[3] Upreti, Himanshu, Alok Kumar Pandey, Ziya Uddin, and Manoj Kumar. "Thermophoresis and Brownian motion effects on 3D flow of Casson nanofluid consisting microorganisms over a Riga plate using PSO: A numerical study." *Chinese Journal of Physics* 78 (2022): 234-270. http://dx.doi.org/10.1016/j.cjph.2022.06.019
[4] Ibrahim, Wubshet, and O. D. Makinde. "Magnetohydrodynamic stagnation point flow and heat transfer of Casson nanofluid past a stretching sheet with slip and convective boundary condition." *Journal of Aerospace Engineering* 29, no. 2 (2016): 04015037. http://dx.doi.org/10.1061/(ASCE)AS.1943-5525.0000529
[5] Noranuar, Wan Nura'in Nabilah, Ahmad Qushairi Mohamad, Lim Yeou Jiann, Sharidan Shafie, and Mohd Anuar Jamaludin. "Analytical Solution for MHD Casson Nanofluid Flow and Heat Transfer due to Stretching Sheet in Porous Medium." *Journal of Advanced Research in Numerical Heat Transfer* 19, no. 1 (2024): 43-59. https://doi.org/10.37934/arnht.19.1.4359
[6] Khan, Ansab Azam, Khairy Zaimi, Suliadi Firdaus Sufahani, and Mohammad Ferdows. "MHD flow and heat transfer of double stratified micropolar fluid over a vertical permeable shrinking/stretching sheet with chemical reaction and heat source." *Journal of Advanced Research in Applied Sciences and Engineering Technology* 21, no. 1 (2020): 1-14. https://doi.org/10.37934/araset.21.1.114
[7] Raghunath, Kodi, Mopuri Obulesu, and Konduru Venkateswara Raju. "Radiation absorption on MHD free conduction flow through porous medium over an unbounded vertical plate with heat source." *International Journal of Ambient Energy* 44, no. 1 (2023): 1712-1720. https://doi.org/10.1080/01430750.2023.2181869
[8] Mopuri, Obulesu, A. Sailakumari, Aruna Ganjikunta, E. Sudhakara, K. VenkateswaraRaju, P. Ramesh, Charankumar Ganteda, B. Ramakrishna Reddy, and S. V. K. Varma. "Characteristics of MHD Jeffery Fluid Past an Inclined Vertical Porous Plate." *CFD Letters* 16, no. 6 (2024): 68-89. https://doi.org/10.37934/cfdl.16.6.6889
[9] Reddy, Yanala Dharmendar, Shankar Goud Bejawada, Nek Muhammad Katbar, Ahmed M. Zidan, Wasim Jamshed, Mohamed R. Eid, and Fayza Abdel Aziz ElSeabee. "Heat generating impact on radiative nanofluid flow via exponential expanding surface with convective conditions: Mesh independence examination." *Numerical Heat Transfer, Part A: Applications* (2024): 1-24. https://doi.org/10.1080/10407782.2024.2321523

[10] Vishwanatha, U. B., Y. Dharmendar Reddy, Praveen Barmavatu, and B. Shankar Goud. "Insights into stretching ratio and velocity slip on MHD rotating flow of Maxwell nanofluid over a stretching sheet: Semi-analytical technique OHAM." *Journal of the Indian Chemical Society* 100, no. 3 (2023): 100937. https://doi.org/10.1016/j.jics.2023.100937

[11] Bejawada, Shankar Goud, Yanala Dharmendar Reddy, Wasim Jamshed, Usman, Siti Suzilliana Putri Mohamed Isa, Sayed M. El Din, Kamel Guedri, and M. Israr Ur Rehman. "Comprehensive examination of radiative electromagnetic flowing of nanofluids with viscous dissipation effect over a vertical accelerated plate." *Scientific Reports* 12, no. 1 (2022): 20548. https://doi.org/10.1038/s41598-022-25097-2

[12] Kodi, Raghunath, Obulesu Mopuri, Sujatha Sree, and Venkateswaraju Konduru. "Investigation of MHD Casson fluid flow past a vertical porous plate under the influence of thermal diffusion and chemical reaction." *Heat Transfer* 51, no. 1 (2022): 377-394. http://dx.doi.org/10.1002/htj.22311

[13] Gangadhar, K., T. Kannan, P. Jayalakshmi, and G. Sakthivel. "Dual solutions for MHD Casson fluid over a shrinking sheet with Newtonian heating." *International Journal of Ambient Energy* 42, no. 3 (2021): 331-339. https://doi.org/10.1080/01430750.2018.1550018

[14] Koka, Ramanjana, and Aruna Gajikunta. "Investigating the Impact of Magnetohydrodynamic (MHD) and Radiation on the Casson-Based Nanofluid Flow over a Linear Stretching Sheet in a Porous Medium with Heat Source or Sink." *Journal of Advanced Research in Fluid Mechanics and Thermal Sciences* 111, no. 2 (2023): 170-194. https://doi.org/10.37934/arfmts.111.2.170194

[15] Senapati, Madhusudan, Sampad Kumar Parida, Kharabela Swain, and S. Mohammed Ibrahim. "Analysis of variable magnetic field on chemically dissipative MHD boundary layer flow of Casson fluid over a nonlinearly stretching sheet with slip conditions." *International Journal of Ambient Energy* 43, no. 1 (2022): 3712-3726. https://doi.org/10.1080/01430750.2020.1831601

[16] Malik, M. Y., M. Naseer, S. Nadeem, and Abdul Rehman. "The boundary layer flow of Casson nanofluid over a vertical exponentially stretching cylinder." *Applied Nanoscience* 4 (2014): 869-873. https://doi.org/10.1007/s13204-013-0267-0

[17] Tawade, Jagadish V., C. N. Guled, Samad Noeiaghdam, Unai Fernandez-Gamiz, Vediyappan Govindan, and Sundarappan Balamuralitharan. "Effects of thermophoresis and Brownian motion for thermal and chemically reacting Casson nanofluid flow over a linearly stretching sheet." *Results in Engineering* 15 (2022): 100448. https://doi.org/10.1016/j.rineng.2022.100448

[18] Jamshed, Wasim, G. K. Ramesh, G. S. Roopa, Kottakkaran Sooppy Nisar, Rabia Safdar, J. K. Madhukesh, Faisal Shahzad, Siti Suzilliana Putri Mohamed Isa, B. Shankar Goud, and Mohamed R. Eid. "Electromagnetic radiation and convective slippery stipulation influence in viscous second grade nanofluid through penetrable material." *ZAMM-Journal of Applied Mathematics and Mechanics/Zeitschrift für Angewandte Mathematik und Mechanik* (2022): e202200002. https://doi.org/10.1002/zamm.202200002

[19] Khan, W. A., and I. Pop. "Boundary-layer flow of a nanofluid past a stretching sheet." *International journal of heat and mass transfer* 53, no. 11-12 (2010): 2477-2483. https://doi.org/10.1016/j.ijheatmasstransfer.2010.01.032

[20] Usman, M., Feroz Ahmed Soomro, Rizwan Ul Haq, W. Wang, and Ozlem Defterli. "Thermal and velocity slip effects on Casson nanofluid flow over an inclined permeable stretching cylinder via collocation method." *International Journal of Heat and Mass Transfer* 122 (2018): 1255-1263. http://dx.doi.org/10.1016/j.ijheatmasstransfer.2018.02.045

[21] Bharathi, V., R. Vijayaragavan, and J. Prakash. "Heat and mass transfer effect of a Magnetohydrodynamic Casson fluid flow in the presence of inclined plate." *Indian Journal of Pure & Applied Physics (IJPAP)* 59, no. 1 (2021): 28-39. https://doi.org/10.56042/ijpap.v59i1.33042

[22] Alabdulhadi, Sumayyah, Sakhinah Abu Bakar, Anuar Ishak, Iskandar Waini, and Sameh E. Ahmed. "Effect of buoyancy force on an unsteady thin film flow of Al2O3/water nanofluid over an inclined stretching sheet." *Mathematics* 11, no. 3 (2023): 739. https://doi.org/10.3390/math11030739

[23] Biswal, Manasa M., Bharat K. Swain, Manjula Das, and Gouranga Charan Dash. "Heat and mass transfer in MHD stagnation-point flow toward an inclined stretching sheet embedded in a porous medium." *Heat Transfer* 51, no. 6 (2022): 4837-4857. https://doi.org/10.1002/htj.22525

[24] Barik, Ashok K., Saumya K. Mishra, S. R. Mishra, and P. K. Pattnaik. "Multiple slip effects on MHD nanofluid flow over an inclined, radiative, and chemically reacting stretching sheet by means of FDM." *Heat Transfer—Asian Research* 49, no. 1 (2020): 477-501. https://doi.org/10.1002/htj.21622

[25] Rehman, Sajid, M. Idrees, Rehan Ali Shah, and Zeeshan Khan. "Suction/injection effects on an unsteady MHD Casson thin film flow with slip and uniform thickness over a stretching sheet along variable flow properties." *Boundary Value Problems* 2019 (2019): 1-24. https://doi.org/10.1186/s13661-019-1133-0

[26] Mishra, Manasi, Lipika Panigrahi, and Jayaprakash Panda. "Investigation of induced magnetic field on MHD radiative flow across an exponentially stretching sheet." *International Journal of Ambient Energy* 44, no. 1 (2023): 1192-1201. https://doi.org/10.1080/01430750.2023.2169757

[27] Endalew, Mehari Fentahun. "Analytical study of heat and mass transfer effects on unsteady Casson fluid flow over an oscillating plate with thermal and solutal boundary conditions." *Heat Transfer* 50, no. 6 (2021): 6285-6299. https://doi.org/10.1002/htj.22172

[28] Sarwar, Noman, Muhammad Imran Asjad, Sajjad Hussain, Md Nur Alam, and Mustafa Inc. "Inclined magnetic field and variable viscosity effects on bioconvection of Casson nanofluid slip flow over non linearly stretching sheet." *Propulsion and Power Research* 11, no. 4 (2022): 565-574. https://doi.org/10.1016/j.jppr.2022.09.002

[29] Manvi, Bharatkumar K., Shravankumar B. Kerur, Jagadish V. Tawade, Juan J. Nieto, Sagar Ningonda Sankeshwari, Hijaz Ahmad, and Vediyappan Govindan. "MHD Casson nanofluid boundary layer flow in presence of radiation and non-uniform heat source/sink." *Math. Model. Control* 3 (2023): 152-167. https://doi.org/10.3934/mmc.2023014

[30] Panigrahi, Lipika, Jayaprakash Panda, Kharabela Swain, and Gouranga Charan Dash. "Heat and mass transfer of MHD Casson nanofluid flow through a porous medium past a stretching sheet with Newtonian heating and chemical reaction." *Karbala International Journal of Modern Science* 6, no. 3 (2020): 11. http://dx.doi.org/10.33640/2405-609X.1740

[31] Raza, Ali, Sami Ullah Khan, Kamel Al-Khaled, M. Ijaz Khan, Absar Ul Haq, Fakhirah Alotaibi, A. Mousa Abd Allah, and Sumaira Qayyum. "A fractional model for the kerosene oil and water-based Casson nanofluid with inclined magnetic force." *Chemical Physics Letters* 787 (2022): 139277. http://dx.doi.org/10.1016/j.cplett.2021.139277

[32] Koka, Ramanjana, and Aruna Ganjikunta. "Effect of the Aligned Magnetic Field over a Stretching Sheet through Porous Media in Casson Fluid Flow." *CFD Letters* 16, no. 4 (2024): 16-38. https://doi.org/10.37934/cfdl.16.4.1638

[33] Mahabaleshwar, U. S., T. Maranna, Manoranjan Mishra, M. Hatami, and Bengt Sunden. "Radiation effect on stagnation point flow of Casson nanofluid past a stretching plate/cylinder." *Scientific Reports* 14, no. 1 (2024): 1387. https://doi.org/10.1038/s41598-024-51963-2

[34] Suresh Kumar, Y., Shaik Hussain, K. Raghunath, Farhan Ali, Kamel Guedri, Sayed M. Eldin, and M. Ijaz Khan. "Numerical analysis of magnetohydrodynamics Casson nanofluid flow with activation energy, Hall current and thermal radiation." *Scientific Reports* 13, no. 1 (2023): 4021. https://doi.org/10.1038/s41598-023-28379-5

[35] Noghrehabadi, Aminreza, Rashid Pourrajab, and Mohammad Ghalambaz. "Effect of partial slip boundary condition on the flow and heat transfer of nanofluids past stretching sheet prescribed constant wall temperature." *International Journal of Thermal Sciences* 54 (2012): 253-261. http://dx.doi.org/10.1016/j.ijthermalsci.2011.11.017

[36] Sekhar, P. Raja, S. Sreedhar, S. Mohammed Ibrahim, and P. Vijaya Kumar. "Radiative heat source fluid flow of MHD Casson nanofluid over a non-linear inclined surface with Soret and Dufour effects." *CFD Letters* 15, no. 7 (2023): 42-60. https://doi.org/10.37934/cfdl.15.7.4260

[37] Jayalakshmi, Pothala, Mopuri Obulesu, Charan Kumar Ganteda, Malaraju Changal Raju, Sibyala Vijayakumar Varma, and Giulio Lorenzini. "Heat transfer analysis of sisko fluid flow over a stretching sheet in a conducting field with Newtonian heating and constant heat flux." *Energies* 16, no. 7 (2023): 3183. https://doi.org/10.3390/en16073183

[38] Vyakaranam, Seethamahalakshmi Vyakaranam, Bindu Pathuri, Venkata Ramana Reddy Gurrampati, and Abayomi Samuel Oke. "Flow of Casson Nanofluid Past a Permeable Surface: Effects of Brownian Motion, Thermophoretic Diffusion and Lorenz force." *CFD Letters* 14, no. 12 (2022): 111125-111125.

[39] Roja, P., T. Sankar Reddy, S. M. Ibrahim, Giulio Lorenzini, and Nor Azwadi Che Sidik. "The Effect of thermophoresis on MHD stream of a micropolar liquid through a porous medium with variable heat and mass flux and thermal radiation." *CFD Letters* 14, no. 4 (2022): 118-136. https://doi.org/10.37934/cfdl.14.4.118136

[40] Nagaraja, B., B. J. Gireesha, G. Sowmya, and M. R. Krishnamurthy. "Slip and radiative flow of shape-dependent dusty nanofluid over a melting stretching sheet." *International Journal of Ambient Energy* 43, no. 1 (2022): 4120-4131. https://doi.org/10.1080/01430750.2020.1861094

[41] Odesola, A. S., M. Gbeminiyi Sobamowo, and I. O. Abiala. "Three-dimensional analysis of MHD Casson Carreau Nanofluid flow and heat transfer over a stretching surface embedded in a porous medium under the influences of thermal radiation and temperature-dependent internal heat generation." *Mathematics in Engineering, Science & Aerospace (MESA)* 13, no. 2 (2022). http://nonlinearstudies.com/index.php/mesa/issue/view/201

[42] Hayat, T., S. Asad, and A. Alsaedi. "Flow of Casson fluid with nanoparticles." *Applied Mathematics and Mechanics* 37 (2016): 459-470. https://doi.org/10.1007/s10483-016-2047-9

[43] Ramesh, G. K., B. J. Gireesha, S. A. Shehzad, and F. M. Abbasi. "Analysis of heat transfer phenomenon in magnetohydrodynamic Casson fluid flow through Cattaneo–Christov heat diffusion theory." *Communications in Theoretical Physics* 68, no. 1 (2017): 91. https://10.1088/0253-6102/68/1/91

[44] Reddy, Nalivela Nagi, Dharmendar Reddy Yanala, B. Shankar Goud, and Srinivasa Rao Vempati. "Impact of porosity and radiation on two-dimensional unsteady magnetohydrodynamics heat transfer stagnation point flow with viscous dissipation." *Heat Transfer* 52, no. 5 (2023): 3538-3556. https://doi.org/10.1002/htj.22839

[45] Madhu, Macha, and Naikoti Kishan. "MHD flow and heat transfer of Casson nanofluid over a wedge." *Mechanics & Industry* 18, no. 2 (2017): 210. http://dx.doi.org/10.1051/meca/2016030

[46] Pal, Dulal, Netai Roy, and K. Vajravelu. "Effects of thermal radiation and Ohmic dissipation on MHD Casson nanofluid flow over a vertical non-linear stretching surface using scaling group transformation." *International Journal of Mechanical Sciences* 114 (2016): 257-267. http://dx.doi.org/10.1016/j.ijmecsci.2016.06.002

[47] Al-Mamun, Abdullah, S. M. Arifuzzaman, Sk Reza-E-Rabbi, Umme Sara Alam, Saiful Islam, and Md Shakhaoath Khan. "Numerical simulation of periodic MHD casson nanofluid flow through porous stretching sheet." *SN Applied Sciences* 3, no. 2 (2021): 271. https://doi.org/10.1007/s42452-021-04140-3

[48] Ghadikolaei, S. S., Kh Hosseinzadeh, D. Domiri Ganji, and B. Jafari. "Nonlinear thermal radiation effect on magneto Casson nanofluid flow with Joule heating effect over an inclined porous stretching sheet." *Case studies in thermal engineering* 12 (2018): 176-187. https://doi.org/10.1016/j.csite.2018.04.009

[49] Rafique, K., M. A. Imran, M. I. Anwar, M. Misiran, and A. Ahmadian. "Energy and mass transport of Casson nanofluid flow over a slanted permeable inclined surface." *Journal of Thermal Analysis and Calorimetry* 144 (2021): 2031-2042. http://dx.doi.org/10.1007/s10973-020-10481-9

[50] Bhandari, Anupam, and Pankaj Kumar Mishra. "Heat and radiation absorption effects on Casson nanofluid flow over a stretching cylinder in the presence of chemical reaction through mathematical modeling." *Special Topics & Reviews in Porous Media: An International Journal* 11, no. 2 (2020). http://10.1615/SpecialTopicsRevPorousMedia.2020029260

[51] Patil, Amar B., Pooja P. Humane, Vishwambhar S. Patil, and Govind R. Rajput. "MHD Prandtl nanofluid flow due to convectively heated stretching sheet below the control of chemical reaction with thermal radiation." *International Journal of Ambient Energy* 43, no. 1 (2022): 4310-4322. https://doi.org/10.1080/01430750.2021.1888803

[52] Jain, Shalini, and Ranjana Kumari. "Analysis of Casson Nanofluid Flow and Heat Transfer Across a Non-linear Stretching Sheet Adopting Keller Box Finite Difference Scheme." *International Journal of Applied and Computational Mathematics* 9, no. 6 (2023): 134. https://doi.org/10.1007/s40819-023-01619-y

[53] Kumar, Vasa Vijaya, Mamidi Narsimha Raja Shekar, and Shankar Goud Bejawada. "Heat and Mass Transfer Significance on MHD Flow over a Vertical Porous Plate in the Presence of Chemical Reaction and Heat Generation." *CFD Letters* 16, no. 5 (2024): 9-20. https://doi.org/10.37934/cfdl.16.5.920

[54] Kumar, Vasa Vijaya, MN Raja Shekar, and Shankar Goud Bejawada. "Role of Soret, Dufour Influence on Unsteady MHD Oscillatory Casson Fluid Flow an Inclined Vertical Porous Plate in the Existence of Chemical Reaction." *Journal of Advanced Research in Fluid Mechanics and Thermal Sciences* 110, no. 2 (2023): 157-175. https://doi.org/10.37934/arfmts.110.2.157175

[55] Yusof, Nur Syamila, Siti Khuzaimah Soid, Mohd Rijal Illias, Ahmad Sukri Abd Aziz, and Nor Ain Azeany Mohd Nasir. "Radiative Boundary Layer Flow of Casson Fluid Over an Exponentially Permeable Slippery Riga Plate with Viscous Dissipation." *Journal of Advanced Research in Applied Sciences and Engineering Technology* 21, no. 1 (2020): 41-51. https://doi.org/10.37934/araset.21.1.4151

[56] Alhadhrami, A., C. S. Vishalakshi, B. M. Prasanna, B. R. Sreenivasa, Hassan AH Alzahrani, RJ Punith Gowda, and R. Naveen Kumar. "Numerical simulation of local thermal non-equilibrium effects on the flow and heat transfer of non-Newtonian Casson fluid in a porous media." *Case Studies in Thermal Engineering* 28 (2021): 101483. https://doi.org/10.1016/j.csite.2021.101483

[57] Hsiao, Kai-Long. "Stagnation electrical MHD nanofluid mixed convection with slip boundary on a stretching sheet." *Applied Thermal Engineering* 98 (2016): 850-861. https://doi.org/10.1016/j.applthermaleng.2015.12.138

[58] Yusof, Zanariah Mohd, Noraini Ahmad, and Anuar Jamaludin. "The Effects of Buoyancy, Magnetic Field and Thermal Radiation on the Flow and Heat Transfer due to an Exponentially Stretching Sheet." *CFD Letters* 15, no. 4 (2023): 1-16. https://doi.org/10.37934/cfdl.15.4.116

[59] Umamaheswar, Mummadisetty, Peram Madhu Mohan Reddy, Obulesu Mopuri, Anumula Vidhyullatha, Nakkarasupalli Mallikarjuna Reddy, Ankita Tiwari, Charankumar Ganteda, and Koppula Rama Thulasi. "Analysis of Energy and Mass Transport Flow of Ethyleneglycol (C2H6O2) Based Nanofluid over an Infinite Porous Plate." *Journal of Advanced Research in Fluid Mechanics and Thermal Sciences* 108, no. 1 (2023): 136-157. https://doi.org/10.37934/arfmts.108.1.136157